

Veamy: an extensible object-oriented C++ library for the virtual element method

A. Ortiz-Bernardin^{a,*}, C. Alvarez^{a,b}, N. Hitschfeld-Kahler^b, A. Russo^{c,d},
R. Silva-Valenzuela^a, E. Olate-Sanzana^a

^a*Department of Mechanical Engineering, Universidad de Chile, Av. Beauchef 851, Santiago 8370456, Chile.*

^b*Department of Computer Science (DCC), Universidad de Chile, Av. Beauchef 851, Santiago 8370456, Chile.*

^c*Dipartimento di Matematica e Applicazioni, Università di Milano-Bicocca, 20153 Milano, Italy.*

^d*Istituto di Matematica Applicata e Tecnologie Informatiche del CNR, via Ferrata 1, 27100 Pavia, Italy.*

Abstract

This paper summarizes the development of **Veamy**, an object-oriented C++ library for the virtual element method (VEM) on general polygonal meshes, whose modular design is focused on its extensibility. The two-dimensional linear elastostatic problem has been chosen as the starting stage for the development of this library. The theory of the VEM in which **Veamy** is based upon is presented using a notation and a terminology that resemble the language of the finite element method in engineering analysis. Several examples are provided to demonstrate the usage of **Veamy**, and in particular, one of them features the interaction between **Veamy** and the polygonal mesh generator **PolyMesher**. **Veamy** is free and open source software.

Keywords: virtual element method, polygonal meshes, object-oriented programming, C++

*Corresponding author. Tel: +56 (2) 297 846 64, Fax: +56 (2) 268 960 57,
Email address: aortizb@uchile.cl (A. Ortiz-Bernardin)

1. Introduction

When a boundary-value problem, such as the linear elastostatic problem, is solved numerically using a Galerkin weak formulation, the trial and test displacements are replaced by their discrete representations, which adopt the form of

$$\mathbf{v}^h(\mathbf{x}) = \sum_{a=1}^N \phi_a(\mathbf{x}) \mathbf{v}_a, \quad (1)$$

where $\phi_a(\mathbf{x})$ are nodal basis functions, $\mathbf{v}_a = [v_{1a} \ v_{2a}]^T$ are nodal displacements in the two-dimensional Cartesian coordinate system and N is the number of nodes that define an element. In this paper, we consider basis functions that reproduce linear fields, which is the lowest possible order in the Galerkin weak formulation of the linear elastostatic problem. Due to the nature of some basis functions, these discrete trial and test displacement fields may represent linear fields plus some additional non-polynomial or higher-order terms. Such additional terms cause inhomogeneous deformations, and when present, integration errors appear in the numerical integration of the stiffness matrix leading to stability issues that affect the convergence of the approximation method. This is the case of polygonal and polyhedral finite element methods [13, 29, 31], and meshfree Galerkin methods [4, 5, 7, 9–12, 19–22].

The virtual element method [33] (VEM) has been presented to deal with these integration issues. In short, the method consists in the construction of an algebraic (exact) representation of the stiffness matrix without the explicit evaluation of basis functions (basis functions are *virtual*). The stiffness constructed in such a manner is referred to as *computable* as opposed to the *uncomputable* stiffness that would require evaluation of basis functions derivatives at quadrature points inside the element. In the VEM, the stiffness matrix is decomposed into two parts: a consistent matrix that guarantees the exact reproduction of a linear displacement field and a correction matrix that provides stability. Such a decomposition is formulated in the spirit of the Lax equivalence theorem (consistency + stability \rightarrow convergence) for finite-difference schemes and is sufficient for the method to

pass the patch test [6]. Recently, the virtual element framework has been used to correct integration errors in polygonal finite element methods [14, 18, 36] and in meshfree Galerkin methods [23].

In this paper, object-oriented programming concepts are adopted to develop a C++ library, named **Veamy**, that implements the VEM on general polygonal meshes. The two-dimensional linear elastostatic problem has been chosen as the starting stage for the development of this library. **Veamy** uses Eigen library [15] for linear algebra, and Triangle [26] and Clipper [17] are used for the implementation of its polygonal mesh generator, **Delynoi** [1], which is based on the constrained Voronoi diagram. Despite this in-built polygonal mesh generator, **Veamy** is capable of interacting straightforwardly with **PolyMesher** [30], a polygonal mesh generator that is widely used in the VEM and polygonal finite elements communities. In presenting the theory of the VEM in which **Veamy** is built upon, we adopt a notation and a terminology that resemble the language of the finite element method (FEM) in engineering analysis. The work of Gain et al. [14] is in line with this aim and has inspired most of the notation and terminology used in this paper. We complete the excellent work of Gain et al. by providing some additional theoretical details that are not explicitly given therein.

Veamy is primarily intended for research and teaching purposes with entities commonly found in the VEM and FEM literature such as mesh, degrees of freedom, elements, element stiffness matrix and element force vector, represented by objects. In contrast to some of the well-established free and open source object-oriented FEM codes such as FreeFEM++ [16], FEniCS [2] and Feel++ [24], **Veamy** does not generate code from the variational form of a particular problem, since that kind of implementations tend to hide the intricacies of the method. On the contrary, since **Veamy**'s scope is research and teaching, in its design we wanted a direct and balanced correspondence between theory and implementation. In this sense, **Veamy** is very similar in its spirit to the 50 lines MATLAB implementation of VEM [28]. However, compared to this MATLAB implementation, **Veamy** is an improvement

in the following aspects:

- Its core VEM numerical implementation is entirely built on free and open source libraries.
- It offers the possibility of using a built-in polygonal mesh generator, whose implementation is also entirely built on free and open source libraries. In addition, it allows a straightforward interaction with `PolyMesher` [30], a popular and widely used MATLAB-based polygonal mesh generator.
- It is designed using the object-oriented paradigm, which allows a safer and better code design, facilitates code reuse and recycling, code maintenance, and therefore code extension.
- Its initial release implements the two-dimensional linear elastostatic problem, which gives more insights into the VEM theory and its implementation than the two-dimensional Poisson problem used in the MATLAB implementation [28].

Veamy is free and open source software, and to the best of our knowledge, is the first object-oriented C++ implementation of the VEM.

The remainder of this paper is structured as follows. The boundary-value problem and the Galerkin weak formulation for two-dimensional linear elastostatics are presented in Section 2. Section 3 presents the theoretical aspects of the VEM for the two-dimensional linear elastostatic problem along with the construction of the VEM element stiffness matrix and the VEM element force vector. The general object-oriented structure of **Veamy** is described and explained in Section 4. Several examples that demonstrate the usage of **Veamy** are presented in Section 5. The paper ends with some concluding remarks in Section 6.

2. Model problem

2.1. Linear elastostatic boundary-value problem

Consider an elastic body that occupies the open domain $\Omega \subset \mathbb{R}^2$ and is bounded by the one-dimensional surface Γ whose unit outward normal is \mathbf{n}_Γ . The boundary is assumed to admit decompositions $\Gamma = \Gamma_g \cup \Gamma_f$ and $\emptyset = \Gamma_g \cap \Gamma_f$, where Γ_g is the essential (Dirichlet) boundary and Γ_f is the natural (Neumann) boundary. The closure of the domain is $\overline{\Omega} \equiv \Omega \cup \Gamma$. Let $\mathbf{u}(\mathbf{x}) : \Omega \rightarrow \mathbb{R}^2$ be the displacement field at a point \mathbf{x} of the elastic body when the body is subjected to external tractions $\mathbf{f}(\mathbf{x}) : \Gamma_f \rightarrow \mathbb{R}^2$ and body forces $\mathbf{b}(\mathbf{x}) : \Omega \rightarrow \mathbb{R}^2$. The imposed essential (Dirichlet) boundary conditions are $\mathbf{g}(\mathbf{x}) : \Gamma_g \rightarrow \mathbb{R}^2$. The boundary-value problem for two-dimensional linear elastostatics is: find $\mathbf{u}(\mathbf{x}) : \Omega \rightarrow \mathbb{R}^2$ such that

$$\nabla \cdot \boldsymbol{\sigma} + \mathbf{b} = 0 \quad \forall \mathbf{x} \in \Omega, \quad (2a)$$

$$\mathbf{u} = \mathbf{g} \quad \forall \mathbf{x} \in \Gamma_g, \quad (2b)$$

$$\boldsymbol{\sigma} \cdot \mathbf{n}_\Gamma = \mathbf{f} \quad \forall \mathbf{x} \in \Gamma_f, \quad (2c)$$

where $\boldsymbol{\sigma}$ is the Cauchy stress tensor.

2.2. Galerkin weak formulation

When deriving the Galerkin weak form of the linear elastostatic problem using the method of weighted residuals, with \mathbf{v} being the arbitrary test (weighting) function, the following expression for the bilinear form is obtained:

$$a(\mathbf{u}, \mathbf{v}) = \int_{\Omega} \boldsymbol{\sigma}(\mathbf{u}) : \nabla \mathbf{v} \, d\mathbf{x}. \quad (3)$$

The gradient of the displacement field can be decomposed into its symmetric ($\nabla_S \mathbf{v}$) and skew-symmetric ($\nabla_{AS} \mathbf{v}$) parts, as follows:

$$\nabla \mathbf{v} = \nabla_S \mathbf{v} + \nabla_{AS} \mathbf{v} = \boldsymbol{\varepsilon}(\mathbf{v}) + \boldsymbol{\omega}(\mathbf{v}), \quad (4)$$

where

$$\nabla_S \mathbf{v} = \boldsymbol{\varepsilon}(\mathbf{v}) = \frac{1}{2} (\nabla \mathbf{v} + \nabla^T \mathbf{v}) \quad (5)$$

is known as the strain tensor, and

$$\nabla_{AS} \mathbf{v} = \boldsymbol{\omega}(\mathbf{v}) = \frac{1}{2} (\nabla \mathbf{v} - \nabla^T \mathbf{v}) \quad (6)$$

is the skew-symmetric gradient tensor that represents rotations. Since the stress tensor is symmetric, its product with the skew-symmetric gradient tensor is zero, thereby simplifying the bilinear form to

$$a(\mathbf{u}, \mathbf{v}) = \int_{\Omega} \boldsymbol{\sigma}(\mathbf{u}) : \boldsymbol{\varepsilon}(\mathbf{v}) \, d\mathbf{x}, \quad (7)$$

which leads to the usual form of presenting the weak formulation: find $\mathbf{u}(\mathbf{x}) \in V$ such that

$$a(\mathbf{u}, \mathbf{v}) = \ell_b(\mathbf{v}) + \ell_f(\mathbf{v}) \quad \forall \mathbf{v}(\mathbf{x}) \in W, \quad (8a)$$

$$a(\mathbf{u}, \mathbf{v}) = \int_{\Omega} \boldsymbol{\sigma}(\mathbf{u}) : \boldsymbol{\varepsilon}(\mathbf{v}) \, d\mathbf{x}, \quad (8b)$$

$$\ell_b(\mathbf{v}) = \int_{\Omega} \mathbf{b} \cdot \mathbf{v} \, d\mathbf{x}, \quad \ell_f(\mathbf{v}) = \int_{\Gamma_f} \mathbf{f} \cdot \mathbf{v} \, ds, \quad (8c)$$

where V and W are the displacement trial and test spaces:

$$V := \{ \mathbf{u}(\mathbf{x}) : \mathbf{u} \in [\mathcal{W}(\Omega)]^2 \subseteq [H^1(\Omega)]^2, \mathbf{u} = \mathbf{g} \text{ on } \Gamma_g \},$$

$$W := \{ \mathbf{v}(\mathbf{x}) : \mathbf{v} \in [\mathcal{W}(\Omega)]^2 \subseteq [H^1(\Omega)]^2, \mathbf{v} = \mathbf{0} \text{ on } \Gamma_g \},$$

where the space $\mathcal{W}(\Omega)$ includes linear displacement fields.

The integrals appearing in the Galerkin weak form are, with few exceptions, uncomputable, meaning that in practice the integrals are evaluated at quadrature points in the interior of disjoint non overlapping elements that form a partition of the domain known as mesh. We denote by E an element having an area of $|E|$ and a boundary ∂E that is formed by edges e of length $|e|$. The partition formed by these elements is denoted as \mathcal{T}^h , where h is the maximum diameter of the elements in the partition. The set formed by the

union of all the element edges in this partition is denoted as \mathcal{E}^h , and the set formed by all the element edges lying on Γ_f as \mathcal{E}_f^h . The evaluation of the Galerkin weak form integrals using quadrature points in the interior of an element is, with few exceptions, not exact (errors are introduced) and therefore the bilinear and linear forms are replaced by their approximate and mesh-dependent counterparts:

$$a^h(\mathbf{u}, \mathbf{v}) = \sum_{E \in \mathcal{T}^h} a_E^h(\mathbf{u}, \mathbf{v}), \quad \text{and} \quad \ell_b^h(\mathbf{v}) = \sum_{E \in \mathcal{T}^h} \ell_{b,E}^h(\mathbf{v}) \quad \text{and} \quad \ell_f^h(\mathbf{v}) = \sum_{e \in \mathcal{E}_f^h} \ell_{f,e}^h(\mathbf{v}),$$

respectively. Furthermore, the same partition is used to approximate the trial and test displacement fields, which leads to the usual discrete bilinear and linear forms:

$$a^h(\mathbf{u}^h, \mathbf{v}^h) = \sum_{E \in \mathcal{T}^h} a_E^h(\mathbf{u}^h, \mathbf{v}^h), \quad \text{and} \quad \ell_b^h(\mathbf{v}^h) = \sum_{E \in \mathcal{T}^h} \ell_{b,E}^h(\mathbf{v}^h) \quad \text{and} \quad \ell_f^h(\mathbf{v}^h) = \sum_{e \in \mathcal{E}_f^h} \ell_{f,e}^h(\mathbf{v}^h),$$

respectively, and the corresponding discrete (element-wise) trial and test spaces as:

$$\begin{aligned} V^h &:= \left\{ \mathbf{u}^h(\mathbf{x}) : \mathbf{u}^h \in [\mathcal{W}(E)]^2 \subseteq [H^1(E)]^2 \ \forall E \in \mathcal{T}^h, \ \mathbf{u}^h = \mathbf{g} \text{ on } \Gamma_g^h \right\}, \\ W^h &:= \left\{ \mathbf{v}^h(\mathbf{x}) : \mathbf{v}^h \in [\mathcal{W}(E)]^2 \subseteq [H^1(E)]^2 \ \forall E \in \mathcal{T}^h, \ \mathbf{v}^h = \mathbf{0} \text{ on } \Gamma_g^h \right\}, \end{aligned}$$

where Γ_g^h is the discrete essential boundary, and $V^h \subset V$ and $W^h \subset W$.

3. The virtual element method

In classical two-dimensional finite element methods, the partition \mathcal{T}^h is usually formed by triangles and quadrilaterals. Here, we consider the possibility of using elements with arbitrary number of edges, that is, polygonal elements. So in essence, the partitioning of the domain will be achieved using a polygonal mesh generator. And for these polygonal elements, we will construct their stiffness matrices and nodal force vectors using the theory of the virtual element method.

3.1. The polygonal element

Let the domain Ω be partitioned into disjoint non overlapping polygonal elements of straight edges. We keep the notation for partition and related entities and measures as given in Section 2.2. The number of edges and nodes of a polygonal element are denoted by N . The unit outward normal to the element boundary in the Cartesian coordinate system is denoted as $\mathbf{n} = [n_1 \ n_2]^T$. Fig. 1 presents a schematic representation of a polygonal element for $N = 5$, where the edge e_a of length $|e_a|$ and the edge e_{a-1} of length $|e_{a-1}|$ are the element edges incident to node a , and \mathbf{n}_a and \mathbf{n}_{a-1} are the unit outward normals to these edges, respectively.

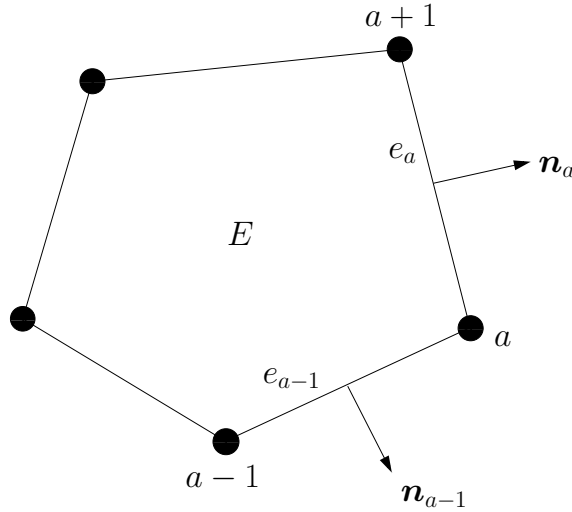


Fig. 1: Schematic representation of a polygonal element of $N = 5$ edges.

3.2. Projection operators

As in finite elements, for the numerical solution to converge monotonically it is required that the displacement approximation in the polygonal element can represent rigid body modes and constant strain states. This requires that the displacement approximation in the element is at least a linear polynomial [27]. We will define projection operators that

allow the extraction of the rigid body modes, the constant strain modes and the linear polynomial part of the motion. In this exposition, the displacement approximation is assumed to be continuous within the element and across inter-element boundaries (i.e. no gaps or cracks open up), which is also a necessary condition for convergence [27].

Consider the following three spaces: the space of rigid body motions (denoted by \mathcal{R}), the space of constant strain states (denoted by \mathcal{C}), and the space of linear displacements (denoted by \mathcal{P}) that are able to represent rigid body motions and states of constant strains.

Since polygonal elements can generally have more than three nodes, we have to consider the possibility that the displacement approximation within a polygonal element is composed of a linear polynomial part plus an additional¹ non-polynomial or higher-order part, which implies that $\mathbf{u}(\mathbf{x}) \in [\mathcal{W}(E)]^2 \supseteq [\mathcal{P}(E)]^2$.

To extract the components of the displacement in the three aforementioned spaces, the following projections are defined:

$$\Pi_{\mathcal{R}} : [\mathcal{W}(E)]^2 \rightarrow [\mathcal{R}(E)]^2, \quad \Pi_{\mathcal{R}} \mathbf{r} = \mathbf{r}, \quad \forall \mathbf{r} \in [\mathcal{R}(E)]^2 \quad (11)$$

for extracting the rigid body motions,

$$\Pi_{\mathcal{C}} : [\mathcal{W}(E)]^2 \rightarrow [\mathcal{C}(E)]^2, \quad \Pi_{\mathcal{C}} \mathbf{c} = \mathbf{c}, \quad \forall \mathbf{c} \in [\mathcal{C}(E)]^2 \quad (12)$$

for extracting the constant strain modes, and

$$\Pi_{\mathcal{P}} : [\mathcal{W}(E)]^2 \rightarrow [\mathcal{P}(E)]^2, \quad \Pi_{\mathcal{P}} \mathbf{p} = \mathbf{p}, \quad \forall \mathbf{p} \in [\mathcal{P}(E)]^2 \quad (13)$$

for extracting the linear polynomial part. These operators are required to satisfy the following orthogonality conditions:

$$\Pi_{\mathcal{R}} \mathbf{c} = \mathbf{0}, \quad \forall \mathbf{c} \in [\mathcal{C}(E)]^2 \quad (14)$$

$$\Pi_{\mathcal{C}} \mathbf{r} = \mathbf{0}, \quad \forall \mathbf{r} \in [\mathcal{R}(E)]^2, \quad (15)$$

¹Just for the lowest order polygon, that is the three-node triangle, the approximation is composed solely of the linear polynomial part. For a four-node quadrilateral finite element, a quadratic monomial exists, which is considered as the additional high-order term in the approximation.

so that elements of \mathcal{C} have no rigid body motions and elements of \mathcal{R} have no constant strain modes, which means that $\Pi_{\mathcal{C}}\Pi_{\mathcal{R}} = \Pi_{\mathcal{R}}\Pi_{\mathcal{C}} = 0$, and thus the projection onto \mathcal{P} can be written as

$$\Pi_{\mathcal{P}} = \Pi_{\mathcal{R}} + \Pi_{\mathcal{C}} \quad (16)$$

and the space of linear displacements as $\mathcal{P} = \mathcal{R} + \mathcal{C}$. In Appendix A, the orthogonality conditions (14) and (15) are verified.

So, any $\mathbf{u}, \mathbf{v} \in [\mathcal{W}(E)]^2$ can be decomposed into three terms, as follows:

$$\mathbf{u} = \Pi_{\mathcal{R}}\mathbf{u} + \Pi_{\mathcal{C}}\mathbf{u} + (\mathbf{u} - \Pi_{\mathcal{P}}\mathbf{u}), \quad (17a)$$

$$\mathbf{v} = \Pi_{\mathcal{R}}\mathbf{v} + \Pi_{\mathcal{C}}\mathbf{v} + (\mathbf{v} - \Pi_{\mathcal{P}}\mathbf{v}), \quad (17b)$$

that is, into a rigid body part, a constant strain part and the remaining non-polynomial or higher-order terms.

3.3. Energy-orthogonality conditions

The crucial point in the VEM is that the displacements (17) once replaced into the bilinear form (7) effectively lead to a split of the stiffness matrix that permits to isolate the non-polynomial or higher-order terms and thus take control over their behavior. The following energy-orthogonality conditions are essentials to this aim.

Consider the bilinear form (7) at the polygonal element level. The projection map $\Pi_{\mathcal{C}}$ is required to satisfy the following condition:

$$a_E(\mathbf{c}, \mathbf{v} - \Pi_{\mathcal{C}}\mathbf{v}) = 0 \quad \forall \mathbf{c} \in [\mathcal{C}(E)]^2, \quad \mathbf{v} \in [\mathcal{W}(E)]^2, \quad (18)$$

which means that $\mathbf{v} - \Pi_{\mathcal{C}}\mathbf{v}$ is energetically orthogonal to \mathcal{C} .

In addition, the following energy-orthogonality condition extends from (18): the projection map $\Pi_{\mathcal{P}}$ satisfies

$$a_E(\mathbf{p}, \mathbf{v} - \Pi_{\mathcal{P}}\mathbf{v}) = 0 \quad \forall \mathbf{p} \in [\mathcal{P}(E)]^2, \quad \mathbf{v} \in [\mathcal{W}(E)]^2, \quad (19)$$

which means that $\mathbf{v} - \Pi_{\mathcal{P}}\mathbf{v}$ is energetically orthogonal to \mathcal{P} . To prove this condition, it is noted that rigid body motions have zero strain, that is, $\boldsymbol{\varepsilon}(\mathbf{r}) = 0 \ \forall \mathbf{r} \in [\mathcal{R}(E)]^2$ and $\boldsymbol{\varepsilon}(\Pi_{\mathcal{R}}\mathbf{v}) = 0$ (these are proved in Appendix A). So basically, any term involving rigid body modes \mathbf{r} and $\Pi_{\mathcal{R}}\mathbf{v}$ in the bilinear form is exactly zero. On using the foregoing observations, the energy-orthogonality condition (19) is proved as follows:

Proof.

$$\begin{aligned} a_E(\mathbf{p}, \mathbf{v} - \Pi_{\mathcal{P}}\mathbf{v}) &= a_E(\mathbf{r} + \mathbf{c}, \mathbf{v} - \Pi_{\mathcal{R}}\mathbf{v} - \Pi_{\mathcal{C}}\mathbf{v}) \\ &= a_E(\mathbf{c}, \mathbf{v} - \Pi_{\mathcal{C}}\mathbf{v}) - a_E(\mathbf{c}, \Pi_{\mathcal{R}}\mathbf{v}) + a_E(\mathbf{r}, \mathbf{v} - \Pi_{\mathcal{R}}\mathbf{v} - \Pi_{\mathcal{C}}\mathbf{v}) \\ &= a_E(\mathbf{c}, \mathbf{v} - \Pi_{\mathcal{C}}\mathbf{v}) = 0, \end{aligned}$$

where (18) has been used in the last equality. \square

A last observation is noted. Since $\mathbf{p} = \mathbf{r} + \mathbf{c}$ and $a_E(\mathbf{r}, \cdot) = 0$, the following energy-orthogonality condition emerges from (19):

$$a_E(\mathbf{c}, \mathbf{v} - \Pi_{\mathcal{P}}\mathbf{v}) = 0 \quad \forall \mathbf{c} \in [\mathcal{C}(E)]^2, \quad \mathbf{v} \in [\mathcal{W}(E)]^2. \quad (20)$$

3.4. The VEM bilinear form

Substituting the VEM decomposition (17) into the bilinear form (7) leads to the following split of the bilinear form at element level:

$$\begin{aligned} a_E(\mathbf{u}, \mathbf{v}) &= a_E(\Pi_{\mathcal{R}}\mathbf{u} + \Pi_{\mathcal{C}}\mathbf{u} + (\mathbf{u} - \Pi_{\mathcal{P}}\mathbf{u}), \Pi_{\mathcal{R}}\mathbf{v} + \Pi_{\mathcal{C}}\mathbf{v} + (\mathbf{v} - \Pi_{\mathcal{P}}\mathbf{v})) \\ &= a_E(\Pi_{\mathcal{C}}\mathbf{u}, \Pi_{\mathcal{C}}\mathbf{v}) + a_E(\mathbf{u} - \Pi_{\mathcal{P}}\mathbf{u}, \mathbf{v} - \Pi_{\mathcal{P}}\mathbf{v}), \end{aligned} \quad (21)$$

where the symmetry of the bilinear form, the fact that $\Pi_{\mathcal{R}}\mathbf{v}$ and $\Pi_{\mathcal{R}}\mathbf{u}$ do not contribute in the bilinear form (both have zero strain), and the energy-orthogonality condition (20) have been invoked.

The first term on the right-hand side of the second line of (21) is the bilinear form associated with the constant strain modes that provides consistency (it leads to the *consistency*

stiffness) and the second term is the bilinear form associated with the non-polynomial or higher-order terms that provides stability (it leads to the *stability* stiffness). We will come back to these concepts later in this section.

3.5. An explicit form of the VEM projection operators

In the preceding section, the projection operators were required to satisfy certain energy-orthogonality conditions. In this section, we use the energy-orthogonality condition (19) to derive the explicit forms of the projection operators.

In order to obtain an explicit form for $\Pi_{\mathcal{R}}$, it is essential to begin the derivations from the bilinear form given in (3) as that expression has the skew-symmetric gradient tensor (see (4)) that represents the rotations of the rigid modes. It is noted that $\boldsymbol{\sigma}(\mathbf{p})$ and $\nabla(\Pi_{\mathcal{P}}\mathbf{v})$ are both constant fields since $\mathbf{p}, \Pi_{\mathcal{P}}\mathbf{v} \in [\mathcal{P}(E)]^2$, thus allowing the following derivation:

$$\begin{aligned} a_E(\mathbf{p}, \mathbf{v} - \Pi_{\mathcal{P}}\mathbf{v}) &= \int_E \boldsymbol{\sigma}(\mathbf{p}) : \nabla(\mathbf{v} - \Pi_{\mathcal{P}}\mathbf{v}) \, d\mathbf{x} \\ &= \boldsymbol{\sigma}(\mathbf{p}) : \left[\int_E \nabla \mathbf{v} \, d\mathbf{x} - \nabla(\Pi_{\mathcal{P}}\mathbf{v}) \int_E d\mathbf{x} \right] \\ &= \boldsymbol{\sigma}(\mathbf{p}) : \left[\int_E \nabla \mathbf{v} \, d\mathbf{x} - \nabla(\Pi_{\mathcal{P}}\mathbf{v})|E| \right]. \end{aligned} \quad (22)$$

And since (22) is required to be exactly zero, it leads to

$$\nabla(\Pi_{\mathcal{P}}\mathbf{v}) = \frac{1}{|E|} \int_E \nabla \mathbf{v} \, d\mathbf{x}. \quad (23)$$

On using (4), Eq. (23) can be further developed, as follows:

$$\nabla(\Pi_{\mathcal{P}}\mathbf{v}) = \frac{1}{|E|} \int_E \boldsymbol{\varepsilon}(\mathbf{v}) \, d\mathbf{x} + \frac{1}{|E|} \int_E \boldsymbol{\omega}(\mathbf{v}) \, d\mathbf{x}, \quad (24)$$

where it is shown that $\nabla(\Pi_{\mathcal{P}}\mathbf{v})$ is equal to the sum of the volume-average of the strain tensor, which we denote as $\widehat{\boldsymbol{\varepsilon}}(\mathbf{v})$, and the volume-average of the skew-symmetric gradient tensor, which we denote as $\widehat{\boldsymbol{\omega}}(\mathbf{v})$, respectively. On appealing to the divergence theorem, the computation of these two volume-averaged tensors is performed on the element boundary, as follows:

$$\widehat{\boldsymbol{\varepsilon}}(\mathbf{v}) = \frac{1}{|E|} \int_E \boldsymbol{\varepsilon}(\mathbf{v}) \, d\mathbf{x} = \frac{1}{2|E|} \int_{\partial E} (\mathbf{v} \otimes \mathbf{n} + \mathbf{n} \otimes \mathbf{v}) \, d\mathbf{s} \quad (25)$$

and

$$\widehat{\boldsymbol{\omega}}(\mathbf{v}) = \frac{1}{|E|} \int_E \boldsymbol{\omega}(\mathbf{v}) \, d\mathbf{x} = \frac{1}{2|E|} \int_{\partial E} (\mathbf{v} \otimes \mathbf{n} - \mathbf{n} \otimes \mathbf{v}) \, ds. \quad (26)$$

Then from (24), $\Pi_{\mathcal{P}}\mathbf{v}$ must have the following form:

$$\Pi_{\mathcal{P}}\mathbf{v} = \widehat{\boldsymbol{\varepsilon}}(\mathbf{v}) \cdot \mathbf{x} + \widehat{\boldsymbol{\omega}}(\mathbf{v}) \cdot \mathbf{x} + a_0. \quad (27)$$

And since a_0 is a constant, this means that the projection $a_E(\mathbf{p}, \mathbf{v} - \Pi_{\mathcal{P}}\mathbf{v}) = 0$ defines $\Pi_{\mathcal{P}}\mathbf{v}$ only up to a constant. Thus, to find a_0 we need a projection operator onto constants such that

$$\Pi_0(\mathbf{v} - \Pi_{\mathcal{P}}\mathbf{v}) = 0 \quad \text{or} \quad \Pi_0(\Pi_{\mathcal{P}}\mathbf{v}) = \Pi_0\mathbf{v}. \quad (28)$$

In Ref. [35], a general expression for $\Pi_0\mathbf{v}$ is chosen as

$$\Pi_0\mathbf{v} = \widehat{\mathbf{v}}(\mathbf{x}) = \frac{1}{|E|} \int_E \mathbf{v}(\mathbf{x}) \, d\mathbf{x}. \quad (29)$$

If the centroid of the polygon is joined to the midpoint of each edge of the polygon by line segments, a representative nodal area (denoted by $|E|_J$) results as the region formed by a node, the midpoint of edges incident to the node, and the centroid of the polygon. With this, the volume integral in (29) can be computed approximately using nodal quadrature with $|E|_J$ as the nodal weight. In fact, this is a typical approach for linear fields in the VEM literature [14, 18, 33–35] and leads to

$$\Pi_0\mathbf{v} \approx \frac{1}{|E|} \sum_{J=1}^N \mathbf{v}(\mathbf{x}_J) |E|_J = \frac{1}{N} \sum_{J=1}^N \mathbf{v}(\mathbf{x}_J) = \overline{\mathbf{v}}, \quad (30)$$

where N is the number of nodes of coordinates \mathbf{x}_J that define the polygonal element. Therefore, Eq. (30) is the mean value of \mathbf{v} over the nodes of the polygonal element. In Appendix A, it is demonstrated that (30) satisfies the orthogonality condition (28).

Applying (28) to (27) gives

$$\Pi_0(\Pi_{\mathcal{P}}\mathbf{v}) = \widehat{\boldsymbol{\varepsilon}}(\mathbf{v}) \cdot \Pi_0\mathbf{x} + \widehat{\boldsymbol{\omega}}(\mathbf{v}) \cdot \Pi_0\mathbf{x} + \Pi_0a_0 = \Pi_0\mathbf{v}. \quad (31)$$

Due to (30), $\Pi_0 a_0 = a_0$, $\Pi_0 \mathbf{v} = \bar{\mathbf{v}}$ and $\Pi_0 \mathbf{x} = \bar{\mathbf{x}}$ ($\bar{\mathbf{x}}$ is equal to the centroid of the polygonal element), which after substituting them into (31) and solving for a_0 gives

$$a_0 = \bar{\mathbf{v}} - \hat{\boldsymbol{\varepsilon}}(\mathbf{v}) \cdot \bar{\mathbf{x}} - \hat{\boldsymbol{\omega}}(\mathbf{v}) \cdot \bar{\mathbf{x}}. \quad (32)$$

Finally, substituting (32) into (27) yields

$$\Pi_{\mathcal{P}} \mathbf{v} = \hat{\boldsymbol{\varepsilon}}(\mathbf{v}) \cdot (\mathbf{x} - \bar{\mathbf{x}}) + \hat{\boldsymbol{\omega}}(\mathbf{v}) \cdot (\mathbf{x} - \bar{\mathbf{x}}) + \bar{\mathbf{v}}. \quad (33)$$

It is immediate from (33) that the projection of \mathbf{v} onto the space of rigid body motions is given by the sum of the rotation mode and the translation mode, respectively, as follows:

$$\Pi_{\mathcal{R}} \mathbf{v} = \hat{\boldsymbol{\omega}}(\mathbf{v}) \cdot (\mathbf{x} - \bar{\mathbf{x}}) + \bar{\mathbf{v}}, \quad (34)$$

and that the projection of \mathbf{v} onto the space of constant strain states is

$$\Pi_{\mathcal{C}} \mathbf{v} = \hat{\boldsymbol{\varepsilon}}(\mathbf{v}) \cdot (\mathbf{x} - \bar{\mathbf{x}}). \quad (35)$$

In Appendix A, it is demonstrated that (35) satisfies (18).

3.6. Another form of the VEM projection operators

At this point we have obtained three important VEM projection operators. A projection operator onto the space of constant strain modes, a projection operator onto the space of rigid body modes, and the sum of both that defines a third projection operator onto the space of linear displacements.

In this section, an alternative form of the VEM projection operators are developed in terms of their space basis. These derivations are very important for the construction of the VEM element matrices. Thus, we need to find the basis for the space of rigid body motions and the basis for the space of constant strain states. These can be derived from the expressions given in (34) and (35). To this end, consider the two-dimensional Cartesian space and the skew-symmetry of $\hat{\boldsymbol{\omega}} \equiv \hat{\boldsymbol{\omega}}(\mathbf{v})$ ². The projection operator (34) can be written

²Note that $\hat{\omega}_{11} = \hat{\omega}_{22} = 0$ and $\hat{\omega}_{21} = -\hat{\omega}_{12}$.

as follows:

$$\begin{aligned}
\Pi_{\mathcal{R}}\mathbf{v} &= \begin{bmatrix} \bar{v}_1 + (x_2 - \bar{x}_2)\hat{\omega}_{12} \\ \bar{v}_2 - (x_1 - \bar{x}_1)\hat{\omega}_{12} \end{bmatrix} \\
&= \begin{bmatrix} 1 & 0 & (x_2 - \bar{x}_2) \\ 0 & 1 & -(x_1 - \bar{x}_1) \end{bmatrix} \begin{bmatrix} \bar{v}_1 \\ \bar{v}_2 \\ \hat{\omega}_{12} \end{bmatrix} \\
&= \begin{bmatrix} 1 \\ 0 \end{bmatrix} \bar{v}_1 + \begin{bmatrix} 0 \\ 1 \end{bmatrix} \bar{v}_2 + \begin{bmatrix} (x_2 - \bar{x}_2) \\ -(x_1 - \bar{x}_1) \end{bmatrix} \hat{\omega}_{12} \\
&= \mathbf{r}_1 \bar{v}_1 + \mathbf{r}_2 \bar{v}_2 + \mathbf{r}_3 \hat{\omega}_{12}.
\end{aligned} \tag{36}$$

Thus, the basis for the space of rigid body modes is:

$$\mathbf{r}_1 = \begin{bmatrix} 1 & 0 \end{bmatrix}^T, \quad \mathbf{r}_2 = \begin{bmatrix} 0 & 1 \end{bmatrix}^T, \quad \mathbf{r}_3 = \begin{bmatrix} (x_2 - \bar{x}_2) & -(x_1 - \bar{x}_1) \end{bmatrix}^T. \tag{37}$$

Similarly, on considering the symmetry of $\hat{\varepsilon} \equiv \hat{\varepsilon}(\mathbf{v})$, the projection operator (35) can be written as

$$\begin{aligned}
\Pi_{\mathcal{C}}\mathbf{v} &= \begin{bmatrix} (x_1 - \bar{x}_1)\hat{\varepsilon}_{11} + (x_2 - \bar{x}_2)\hat{\varepsilon}_{12} \\ (x_1 - \bar{x}_1)\hat{\varepsilon}_{12} + (x_2 - \bar{x}_2)\hat{\varepsilon}_{22} \end{bmatrix} \\
&= \begin{bmatrix} (x_1 - \bar{x}_1) & 0 & (x_2 - \bar{x}_2) \\ 0 & (x_2 - \bar{x}_2) & (x_1 - \bar{x}_1) \end{bmatrix} \begin{bmatrix} \hat{\varepsilon}_{11} \\ \hat{\varepsilon}_{22} \\ \hat{\varepsilon}_{12} \end{bmatrix} \\
&= \begin{bmatrix} (x_1 - \bar{x}_1) \\ 0 \end{bmatrix} \hat{\varepsilon}_{11} + \begin{bmatrix} 0 \\ (x_2 - \bar{x}_2) \end{bmatrix} \hat{\varepsilon}_{22} + \begin{bmatrix} (x_2 - \bar{x}_2) \\ (x_1 - \bar{x}_1) \end{bmatrix} \hat{\varepsilon}_{12} \\
&= \mathbf{c}_1 \hat{\varepsilon}_{11} + \mathbf{c}_2 \hat{\varepsilon}_{22} + \mathbf{c}_3 \hat{\varepsilon}_{12}.
\end{aligned} \tag{38}$$

Thus, the basis for the space of constant strain states is:

$$\mathbf{c}_1 = \begin{bmatrix} (x_1 - \bar{x}_1) & 0 \end{bmatrix}^T, \quad \mathbf{c}_2 = \begin{bmatrix} 0 & (x_2 - \bar{x}_2) \end{bmatrix}^T, \quad \mathbf{c}_3 = \begin{bmatrix} (x_2 - \bar{x}_2) & (x_1 - \bar{x}_1) \end{bmatrix}^T. \tag{39}$$

3.7. Projection matrices

On each polygonal element of N edges, the discrete trial and test displacements are given as

$$\mathbf{u}^h(\mathbf{x}) = \sum_{a=1}^N \phi_a(\mathbf{x}) \mathbf{u}_a, \quad \mathbf{v}^h(\mathbf{x}) = \sum_{b=1}^N \phi_b(\mathbf{x}) \mathbf{v}_b, \tag{40}$$

where $\phi_a(\mathbf{x})$ and $\phi_b(\mathbf{x})$ are nodal basis functions, and $\mathbf{u}_a = [u_{1a} \ u_{2a}]^T$ and $\mathbf{v}_b = [v_{1b} \ v_{2b}]^T$ are nodal displacements in the two-dimensional Cartesian coordinate system. The nodal basis functions are also used for the discretization of the components of the basis for the space of rigid body motions:

$$\mathbf{r}_\alpha^h(\mathbf{x}) = \sum_{a=1}^N \phi_a(\mathbf{x}) \mathbf{r}_\alpha(\mathbf{x}_a), \quad \alpha = 1, \dots, 3 \quad (41)$$

and the components of the basis for the space of constant strain modes:

$$\mathbf{c}_\beta^h(\mathbf{x}) = \sum_{a=1}^N \phi_a(\mathbf{x}) \mathbf{c}_\beta(\mathbf{x}_a), \quad \beta = 1, \dots, 3. \quad (42)$$

The discrete version of the projection map to extract the rigid body motions is obtained by substituting (40) and (41) into (36), which yields

$$\begin{aligned} \left(\Pi_{\mathcal{R}} \mathbf{v}^h \right)_{ab} &= \left[\phi_a \begin{bmatrix} 1 \\ 0 \end{bmatrix} \quad \phi_a \begin{bmatrix} 0 \\ 1 \end{bmatrix} \quad \phi_a \begin{bmatrix} (x_{2a} - \bar{x}_2) \\ -(x_{1a} - \bar{x}_1) \end{bmatrix} \right] \begin{bmatrix} \bar{\phi}_b v_{1b} \\ \bar{\phi}_b v_{2b} \\ q_{2b} v_{1b} - q_{1b} v_{2b} \end{bmatrix} \\ &= \begin{bmatrix} \phi_a & 0 \\ 0 & \phi_a \end{bmatrix} \begin{bmatrix} 1 & 0 & (x_{2a} - \bar{x}_2) \\ 0 & 1 & -(x_{1a} - \bar{x}_1) \end{bmatrix} \begin{bmatrix} \bar{\phi}_b & 0 \\ 0 & \bar{\phi}_b \\ q_{2b} & -q_{1b} \end{bmatrix} \begin{bmatrix} v_{1b} \\ v_{2b} \end{bmatrix}, \end{aligned} \quad (43)$$

where

$$q_{ia} = \frac{1}{2|E|} \int_{\partial E} \phi_a n_i \, ds, \quad i = 1, 2 \quad (44)$$

appeared because of the discretization of $\widehat{\omega}_{12}$ (see (26)). The matrix form of (43) is obtained by expanding the nodal indexes, as follows:

$$\Pi_{\mathcal{R}} \mathbf{v}^h = \sum_{a=1}^N \sum_{b=1}^N \left(\Pi_{\mathcal{R}} \mathbf{v}^h \right)_{ab} = \mathbf{N} \mathbf{P}_{\mathcal{R}} \mathbf{q}, \quad (45)$$

where

$$\mathbf{N} = [(\mathbf{N})_1 \quad \dots \quad (\mathbf{N})_a \quad \dots \quad (\mathbf{N})_N]; \quad (\mathbf{N})_a = \begin{bmatrix} \phi_a & 0 \\ 0 & \phi_a \end{bmatrix}, \quad (46)$$

$$\mathbf{q} = [\mathbf{v}_1^T \quad \dots \quad \mathbf{v}_a^T \quad \dots \quad \mathbf{v}_N^T]^T; \quad \mathbf{v}_a = [v_{1a} \ v_{2a}]^T \quad (47)$$

and

$$\mathbf{P}_{\mathcal{R}} = \mathbf{H}_{\mathcal{R}} \mathbf{W}_{\mathcal{R}}^{\mathbf{T}} \quad (48)$$

with

$$\mathbf{H}_{\mathcal{R}} = \begin{bmatrix} (\mathbf{H}_{\mathcal{R}})_1 \\ \vdots \\ (\mathbf{H}_{\mathcal{R}})_a \\ \vdots \\ (\mathbf{H}_{\mathcal{R}})_N \end{bmatrix}, \quad (\mathbf{H}_{\mathcal{R}})_a = \begin{bmatrix} 1 & 0 \\ 0 & 1 \\ (x_{2a} - \bar{x}_2) & -(x_{1a} - \bar{x}_1) \end{bmatrix}^{\mathbf{T}} \quad (49)$$

and

$$\mathbf{W}_{\mathcal{R}} = \begin{bmatrix} (\mathbf{W}_{\mathcal{R}})_1 \\ \vdots \\ (\mathbf{W}_{\mathcal{R}})_a \\ \vdots \\ (\mathbf{W}_{\mathcal{R}})_N \end{bmatrix}, \quad (\mathbf{W}_{\mathcal{R}})_a = \begin{bmatrix} \bar{\phi}_a & 0 \\ 0 & \bar{\phi}_a \\ q_{2a} & -q_{1a} \end{bmatrix}^{\mathbf{T}}. \quad (50)$$

Similarly, on substituting (40) and (42) into (38) leads to the following discrete version of the projection map to extract the constant strain modes:

$$\begin{aligned} \left(\Pi_C \mathbf{v}^h \right)_{ab} &= \begin{bmatrix} \phi_a \begin{bmatrix} (x_{1a} - \bar{x}_1) \\ 0 \end{bmatrix} & \phi_a \begin{bmatrix} 0 \\ (x_{2a} - \bar{x}_2) \end{bmatrix} & \phi_a \begin{bmatrix} (x_{2a} - \bar{x}_2) \\ (x_{1a} - \bar{x}_1) \end{bmatrix} \end{bmatrix} \\ &\quad \times \begin{bmatrix} 2q_{1b}v_{1b} \\ 2q_{2b}v_{2b} \\ q_{2b}v_{1b} + q_{1b}v_{2b} \end{bmatrix} \\ &= \begin{bmatrix} \phi_a & 0 \\ 0 & \phi_a \end{bmatrix} \begin{bmatrix} (x_{1a} - \bar{x}_1) & 0 & (x_{2a} - \bar{x}_2) \\ 0 & (x_{2a} - \bar{x}_2) & (x_{1a} - \bar{x}_1) \end{bmatrix} \begin{bmatrix} 2q_{1b} & 0 \\ 0 & 2q_{2b} \\ q_{2b} & q_{1b} \end{bmatrix} \\ &\quad \times \begin{bmatrix} v_{1b} \\ v_{2b} \end{bmatrix}. \end{aligned} \quad (51)$$

The matrix form of (51) is obtained by expanding the nodal indexes, as follows:

$$\Pi_C \mathbf{v}^h = \sum_{a=1}^N \sum_{b=1}^N \left(\Pi_C \mathbf{v}^h \right)_{ab} = \mathbf{N} \mathbf{P}_C \mathbf{q}, \quad (52)$$

where

$$\mathbf{P}_C = \mathbf{H}_C \mathbf{W}_C^{\mathbf{T}} \quad (53)$$

with

$$\mathbf{H}_C = \begin{bmatrix} (\mathbf{H}_C)_1 \\ \vdots \\ (\mathbf{H}_C)_a \\ \vdots \\ (\mathbf{H}_C)_N \end{bmatrix}, \quad (\mathbf{H}_C)_a = \begin{bmatrix} (x_{1a} - \bar{x}_1) & 0 \\ 0 & (x_{2a} - \bar{x}_2) \\ (x_{2a} - \bar{x}_2) & (x_{1a} - \bar{x}_1) \end{bmatrix}^T \quad (54)$$

and

$$\mathbf{W}_C = \begin{bmatrix} (\mathbf{W}_C)_1 \\ \vdots \\ (\mathbf{W}_C)_a \\ \vdots \\ (\mathbf{W}_C)_N \end{bmatrix}, \quad (\mathbf{W}_C)_a = \begin{bmatrix} 2q_{1a} & 0 \\ 0 & 2q_{2a} \\ q_{2a} & q_{1a} \end{bmatrix}^T. \quad (55)$$

The matrix form of the projection to extract the polynomial part of the displacement field is then $\mathbf{P}_P = \mathbf{P}_R + \mathbf{P}_C$.

In order to develop the element *consistency* stiffness matrix, it is useful to have the following alternative expression for the discrete projection map to extract the constant strain modes:

$$\begin{aligned} \Pi_C \mathbf{v}^h &= \mathbf{c}_1 \sum_{b=1}^N 2q_{1b} v_{1b} + \mathbf{c}_2 \sum_{b=1}^N 2q_{2b} v_{2b} + \mathbf{c}_3 \sum_{b=1}^N (q_{2b} v_{1b} + q_{1b} v_{2b}) \\ &= \sum_{b=1}^N \begin{bmatrix} 2q_{1b} \mathbf{c}_1 + q_{2b} \mathbf{c}_3 & 2q_{2b} \mathbf{c}_2 + q_{1b} \mathbf{c}_3 \end{bmatrix} \begin{bmatrix} v_{1b} \\ v_{2b} \end{bmatrix} \\ &= \begin{bmatrix} \mathbf{c}_1 & \mathbf{c}_2 & \mathbf{c}_3 \end{bmatrix} \sum_{b=1}^N \begin{bmatrix} 2q_{1b} & 0 \\ 0 & 2q_{2b} \\ q_{2b} & q_{1b} \end{bmatrix} \begin{bmatrix} v_{1b} \\ v_{2b} \end{bmatrix} \\ &= \mathbf{c} \mathbf{W}_C^T \mathbf{q}. \end{aligned} \quad (56)$$

Finally, the discrete version of the projection map onto constants (Eq. (30)) is given as follows:

$$\begin{aligned} (\Pi_0 \mathbf{v}^h)_a &= \frac{1}{N} \sum_{I=1}^N \begin{bmatrix} \phi_a(\mathbf{x}_I) & 0 \\ 0 & \phi_a(\mathbf{x}_I) \end{bmatrix} \begin{bmatrix} v_{1a} \\ v_{2a} \end{bmatrix} \\ &= \begin{bmatrix} \bar{\phi}_a & 0 \\ 0 & \bar{\phi}_a \end{bmatrix} \begin{bmatrix} v_{1a} \\ v_{2a} \end{bmatrix}. \end{aligned} \quad (57)$$

The matrix form of (57) is obtained by expanding the nodal indexes as

$$\Pi_0 \mathbf{v}^h = \sum_{a=1}^N \left(\Pi_0 \mathbf{v}^h \right)_a = \overline{\mathbf{N}} \mathbf{q}, \quad (58)$$

where

$$\overline{\mathbf{N}} = [(\overline{\mathbf{N}})_1 \quad \cdots \quad (\overline{\mathbf{N}})_a \quad \cdots \quad (\overline{\mathbf{N}})_N] ; \quad (\overline{\mathbf{N}})_a = \begin{bmatrix} \overline{\phi}_a & 0 \\ 0 & \overline{\phi}_a \end{bmatrix}. \quad (59)$$

In the VEM, the basis functions are chosen such that on the element boundary they are piecewise linear (edge by edge) and continuous, and therefore they possess the Kronecker-delta property, which permits the following simpler computations:

$$\overline{\phi}_a = \frac{1}{N} \sum_{J=1}^N \phi_a(\mathbf{x}_J) = \frac{1}{N}, \quad (60)$$

where (30) has been used, and an exact evaluation of the integral over the boundary of the element (see (44) and Fig. 1) using a trapezoidal rule, which yields [18, 35]

$$\int_{\partial E} \phi_a n_i \, ds = \frac{1}{2} (|e_{a-1}| \{n_i\}_{a-1} + |e_a| \{n_i\}_a), \quad i = 1, 2. \quad (61)$$

3.8. VEM element stiffness matrix

The decomposition given in (21) provides a means to express the approximate and mesh-dependent bilinear form $a_E^h(\mathbf{u}, \mathbf{v})$ in a way that is computable at the element level, that is,

$$a_E^h(\mathbf{u}, \mathbf{v}) := a_E(\Pi_{\mathcal{C}} \mathbf{u}, \Pi_{\mathcal{C}} \mathbf{v}) + a_E(\mathbf{u} - \Pi_{\mathcal{P}} \mathbf{u}, \mathbf{v} - \Pi_{\mathcal{P}} \mathbf{v}), \quad (62)$$

where its right-hand side, as it will be revealed in the sequel, is computed algebraically. The decomposition (62) has been proved to be endowed with the following crucial properties for establishing convergence [33, 34]:

For all h and for all E in \mathcal{T}^h

- *Consistency:* $\forall \mathbf{p} \in [\mathcal{P}(E)]^2, \forall \mathbf{v}^h \in V^h$

$$a_E^h(\mathbf{p}, \mathbf{v}^h) = a_E(\mathbf{p}, \mathbf{v}^h). \quad (63)$$

- *Stability*: \exists two constants $\alpha_* > 0$ and $\alpha^* > 0$, independent of h and of E , such that

$$\forall \mathbf{v}^h \in V^h \quad \alpha_* a_E(\mathbf{v}^h, \mathbf{v}^h) \leq a_E^h(\mathbf{v}^h, \mathbf{v}^h) \leq \alpha^* a_E(\mathbf{v}^h, \mathbf{v}^h). \quad (64)$$

To obtain the discrete version of the VEM bilinear form (62), the discrete operators $\Pi_{\mathcal{R}} \mathbf{v}^h$ (Eq. (45)), $\Pi_{\mathcal{C}} \mathbf{v}^h$ (Eq. (52)) and $\Pi_{\mathcal{P}} \mathbf{v}^h = \Pi_{\mathcal{R}} \mathbf{v}^h + \Pi_{\mathcal{C}} \mathbf{v}^h$ are used, which yields

$$\begin{aligned} a_E^h(\mathbf{u}^h, \mathbf{v}^h) &= a_E(\mathbf{c} \mathbf{W}_{\mathcal{C}}^T \mathbf{d}, \mathbf{c} \mathbf{W}_{\mathcal{C}}^T \mathbf{q}) + a_E(\mathbf{N} \mathbf{d} - \mathbf{N} \mathbf{P}_{\mathcal{P}} \mathbf{d}, \mathbf{N} \mathbf{q} - \mathbf{N} \mathbf{P}_{\mathcal{P}} \mathbf{q}) \\ &= \mathbf{q}^T \mathbf{W}_{\mathcal{C}} a_E(\mathbf{c}^T, \mathbf{c}) \mathbf{W}_{\mathcal{C}}^T \mathbf{d} + \mathbf{q}^T (\mathbf{I}_{2N} - \mathbf{P}_{\mathcal{P}})^T a_E(\mathbf{N}^T, \mathbf{N}) (\mathbf{I}_{2N} - \mathbf{P}_{\mathcal{P}}) \mathbf{d} \\ &= \mathbf{q}^T |E| \mathbf{W}_{\mathcal{C}} \mathbf{D} \mathbf{W}_{\mathcal{C}}^T \mathbf{d} + \mathbf{q}^T (\mathbf{I}_{2N} - \mathbf{P}_{\mathcal{P}})^T \mathbf{K}_E (\mathbf{I}_{2N} - \mathbf{P}_{\mathcal{P}}) \mathbf{d}, \end{aligned} \quad (65)$$

where \mathbf{I}_{2N} is the identity ($2N \times 2N$) matrix, \mathbf{d} is the column vector of nodal displacements, and $\mathbf{K}_E = a_E(\mathbf{N}^T, \mathbf{N})$ is the standard element stiffness matrix that arises from the discretization of (7) with the field approximation (40) and is in general not computable. On using Voigt notation and observing that $\boldsymbol{\varepsilon}(\mathbf{c}) = [\varepsilon_{11}(\mathbf{c}) \quad \varepsilon_{22}(\mathbf{c}) \quad \varepsilon_{12}(\mathbf{c})]^T = \mathbf{I}_3$ (the identity (3×3) matrix), in (65) we have used that $a_E(\mathbf{c}^T, \mathbf{c}) = \int_E \boldsymbol{\varepsilon}^T(\mathbf{c}) \mathbf{D} \boldsymbol{\varepsilon}(\mathbf{c}) d\mathbf{x} = \mathbf{D} \int_E d\mathbf{x} = |E| \mathbf{D}$, where \mathbf{D} is the constitutive matrix for an isotropic linear elastic material given by

$$\mathbf{D} = \frac{E_Y}{(1+\nu)(1-2\nu)} \begin{bmatrix} 1-\nu & \nu & 0 \\ \nu & 1-\nu & 0 \\ 0 & 0 & 2(1-2\nu) \end{bmatrix} \quad (66)$$

for plane strain condition, and

$$\mathbf{D} = \frac{E_Y}{(1-\nu^2)} \begin{bmatrix} 1 & \nu & 0 \\ \nu & 1 & 0 \\ 0 & 0 & 2(1-\nu) \end{bmatrix} \quad (67)$$

for plane stress condition, where E_Y is the Young's modulus and ν is the Poisson's ratio.

The first term on the right-hand side of (65) is the *consistency* part of the VEM bilinear form that provides patch test satisfaction when the solution is a linear displacement field (condition (63) is satisfied). On the other hand, the *stability* part of the VEM bilinear form (second term on the right-hand side of (65)) is dependant on the uncomputable standard element stiffness \mathbf{K}_E , which introduces an issue. In order to observe the issue, we define the

space of non-polynomial or higher-order terms as \mathcal{H} and consider the following equivalence for the stability term in (62):

$$a_E(\mathbf{u} - \Pi_{\mathcal{P}}\mathbf{u}, \mathbf{v} - \Pi_{\mathcal{P}}\mathbf{v}) = s_E(\mathbf{u} - \Pi_{\mathcal{P}}\mathbf{u}, \mathbf{v} - \Pi_{\mathcal{P}}\mathbf{v}), \quad (68)$$

which for $\mathbf{h} \in \mathcal{H}$ yields

$$a_E(\mathbf{h}, \mathbf{h}) = s_E(\mathbf{h}, \mathbf{h}). \quad (69)$$

Clearly, in (69) $s_E(\mathbf{h}, \mathbf{h})$ must be positive definite so that non-polynomial or higher-order deformation modes are not assigned zero strain energy. Thus, the effect of the uncomputable element stiffness \mathbf{K}_E is the possibility of ending up with an element stiffness that is not positive definite on the non-polynomial or higher-order deformation modes. As discussed in Refs. [33, 34], taking $s_E(\mathbf{u} - \Pi_{\mathcal{P}}\mathbf{u}, \mathbf{v} - \Pi_{\mathcal{P}}\mathbf{v})$ as an estimate for $a_E(\mathbf{u} - \Pi_{\mathcal{P}}\mathbf{u}, \mathbf{v} - \Pi_{\mathcal{P}}\mathbf{v})$ that is symmetric positive definite and scales like the exact bilinear form $a_E(\mathbf{u}, \mathbf{v})$, will satisfy property (64). This is equivalent to replacing \mathbf{K}_E in (65) by an approximate but computable symmetric positive definite stiffness, which is denoted by \mathbf{S}_E . There are quite a few possibilities for this approximate stiffness (see for instance Refs. [14, 33, 34]). Herein, we adopt \mathbf{S}_E given as [14]

$$\mathbf{S}_E = \alpha_E \mathbf{I}_{2N}, \quad \alpha_E = \gamma \frac{|E| \text{trace}(\mathbf{D})}{\text{trace}(\mathbf{H}_C^T \mathbf{H}_C)}, \quad (70)$$

where α_E is the scaling parameter and γ is typically set to 1.

The final expression for the VEM element stiffness matrix associated with the polygonal element can be written as the summation of the *consistency* stiffness and the *stability* stiffness, respectively, as follows:

$$\mathbf{K}_E = |E| \mathbf{W}_C \mathbf{D} \mathbf{W}_C^T + (\mathbf{I}_{2N} - \mathbf{P}_{\mathcal{P}})^T \mathbf{S}_E (\mathbf{I}_{2N} - \mathbf{P}_{\mathcal{P}}). \quad (71)$$

Recall that in the VEM approach, Eqs. (60) and (61) are used in the computations; these along with the nodal coordinates \mathbf{x}_a , the centroid $\bar{\mathbf{x}}$ and area $|E|$ of the polygonal element, and the material matrix \mathbf{D} , completely determine the computation of the matrices

\mathbf{W}_C , $\mathbf{P}_P = \mathbf{H}_R \mathbf{W}_R^T + \mathbf{H}_C \mathbf{W}_C^T$, and \mathbf{S}_E , and therefore of the VEM element stiffness (71). In this process, the basis functions are said to be *virtual* in the sense that on the boundary of the element they are piecewise linear (edge by edge) and continuous, but they are not known explicitly inside the element. Furthermore, their behavior on the element boundary permits an algebraic evaluation of the element stiffness thereby avoiding quadrature errors. And acknowledging that inside the element the basis functions are not known explicitly, results in the following usual way of writing the displacement trial space [33, 36]:

$$V^h := \left\{ \mathbf{v}^h \in [H^1(E) \cap C^0(E)]^2 : \Delta \mathbf{v}^h = \mathbf{0} \text{ in } E, \mathbf{v}^h|_e = \mathcal{P}(e) \forall e \in \partial E \right\},$$

which is known as the virtual element space. Note that because of the interpolation property assumed for the approximation on the element boundary, $\mathbf{v}^h \in V^h$ is able to exactly satisfy linear essential boundary conditions.

3.9. VEM element body and traction force vectors

The VEM element body and traction force vectors are developed by discretizing the linear form, as follows:

$$\ell_E^h(\mathbf{v}) = \ell_{b,E}^h(\Pi_R \mathbf{v}^h + \Pi_C \mathbf{v}^h + (\mathbf{v}^h - \Pi_P \mathbf{v}^h)) + \ell_{f,e}^h(\Pi_R \mathbf{v}^h + \Pi_C \mathbf{v}^h + (\mathbf{v}^h - \Pi_P \mathbf{v}^h)). \quad (72)$$

The VEM element body force vector is obtained from the first term on the right-hand side of (72). For a constant body force vector, we write

$$\begin{aligned} \ell_{b,E}^h(\mathbf{v}^h) &= \mathbf{b} \cdot \int_E \left(\Pi_R \mathbf{v}^h + \Pi_C \mathbf{v}^h + (\mathbf{v}^h - \Pi_P \mathbf{v}^h) \right) d\mathbf{x} \\ &= \mathbf{b} \cdot \left(\int_E \Pi_P \mathbf{v}^h d\mathbf{x} + \int_E (\mathbf{v}^h - \Pi_P \mathbf{v}^h) d\mathbf{x} \right) \\ &= \mathbf{b} \cdot \left(|E| \Pi_0(\Pi_P \mathbf{v}^h) + |E| \Pi_0(\mathbf{v}^h - \Pi_P \mathbf{v}^h) \right) \\ &= |E| \mathbf{b} \cdot \Pi_0 \mathbf{v}^h \\ &= \mathbf{q}^T |E| \bar{\mathbf{N}}^T \mathbf{b}, \end{aligned} \quad (73)$$

where (29) has been used to obtain the third line, (28) and (31) to obtain the fourth line, and (58) to obtain the expression on the last line. The VEM element body force vector is then given by

$$\mathbf{f}_{b,E} = |E| \bar{\mathbf{N}}^T \mathbf{b}. \quad (74)$$

The VEM traction force vector is obtained from the second term on the right-hand side of (72). It is similar to the VEM element body force vector but the integral is one dimension lower. Therefore, on considering the polygonal edge as a one dimensional element, the VEM element traction force vector can be computed similarly to the VEM element body force vector, as follows:

$$\mathbf{f}_{f,e} = |e| \bar{\mathbf{N}}_r^T \mathbf{f}, \quad (75)$$

where

$$\bar{\mathbf{N}}_r = \begin{bmatrix} \bar{\phi}_1 & 0 & \bar{\phi}_2 & 0 \\ 0 & \bar{\phi}_1 & 0 & \bar{\phi}_2 \end{bmatrix} = \begin{bmatrix} \frac{1}{N} & 0 & \frac{1}{N} & 0 \\ 0 & \frac{1}{N} & 0 & \frac{1}{N} \end{bmatrix} = \begin{bmatrix} \frac{1}{2} & 0 & \frac{1}{2} & 0 \\ 0 & \frac{1}{2} & 0 & \frac{1}{2} \end{bmatrix} \quad (76)$$

is a matrix related to the two nodes that define the loaded edge of the polygonal element.

4. Object-oriented implementation of VEM in C++

In this section, we introduce **Veamy**, a library that implements the VEM for the two-dimensional linear elastostatic problem using object-oriented programming in C++. In **Veamy**, entities such as elements, degrees of freedom, constraints, among others, are represented by C++ classes.

Veamy uses the following external libraries:

- Triangle [26], which is used to generate a Delaunay triangulation that is later used to construct a Voronoi-based polygonal mesh.
- Clipper [17], an open source freeware library for clipping and offsetting lines and polygons.
- Eigen [15], a C++ template library for linear algebra.

Triangle and Clipper are used in the implementation of **Delynoi** [1], a polygonal mesher that is based on the computation of the constrained Voronoi diagram. Even though this mesher has been developed for **Veamy**, we decided to treat **Delynoi** as an external mesher since mesh generation is beyond the scope of this paper.

Veamy is free and open source software and is available to be downloaded from <http://camlab.cl/research/software/veamy/>. The source code is provided in the folder named “**Veamy**.” A tutorial manual that is aimed to prepare, compile, and run VEM models using **Veamy**, is provided in the folder “**Veamy/docs/**.” All the source code that implements the VEM is provided in the folder “**Veamy/veamy/**” and the subfolders therein. Everything that is used by **Veamy** but is external to it, is provided in the folder “**Veamy/lib/**.” The folder “**Veamy/polymesher/**” contains a MATLAB function that is intended to be called from **PolyMesher** [30] with the purpose of generating a file containing a **PolyMesher** mesh and boundary conditions that is readable by **Veamy**.

Throughout this section we make reference to the folders that contain the different parts of **Veamy**’s source code.

A UML diagram showing the core design of **Veamy** is presented in Fig. 2. An overview of the main components that are shown in this diagram is provided in Section 4.1, and the nodal displacements computation procedure is summarized in Section 4.2.

*4.1. Overview of C++ classes in the **Veamy** library*

*4.1.1. **Veamer***

The class named **Veamer** is in charge of receiving the problem conditions, including the polygonal mesh, the material parameters of the linear elastic solid, and the boundary conditions. **Veamer** initializes the **Elements** and **DOFs** structures, and keeps them as class members delegating to them most of the work. **Veamer** receives a polygonal mesh created in **Delynoi** [1], and provides all the geometric entities that are needed for VEM computations, such as polygon, nodal points, and segments that define the sides of the polygon.

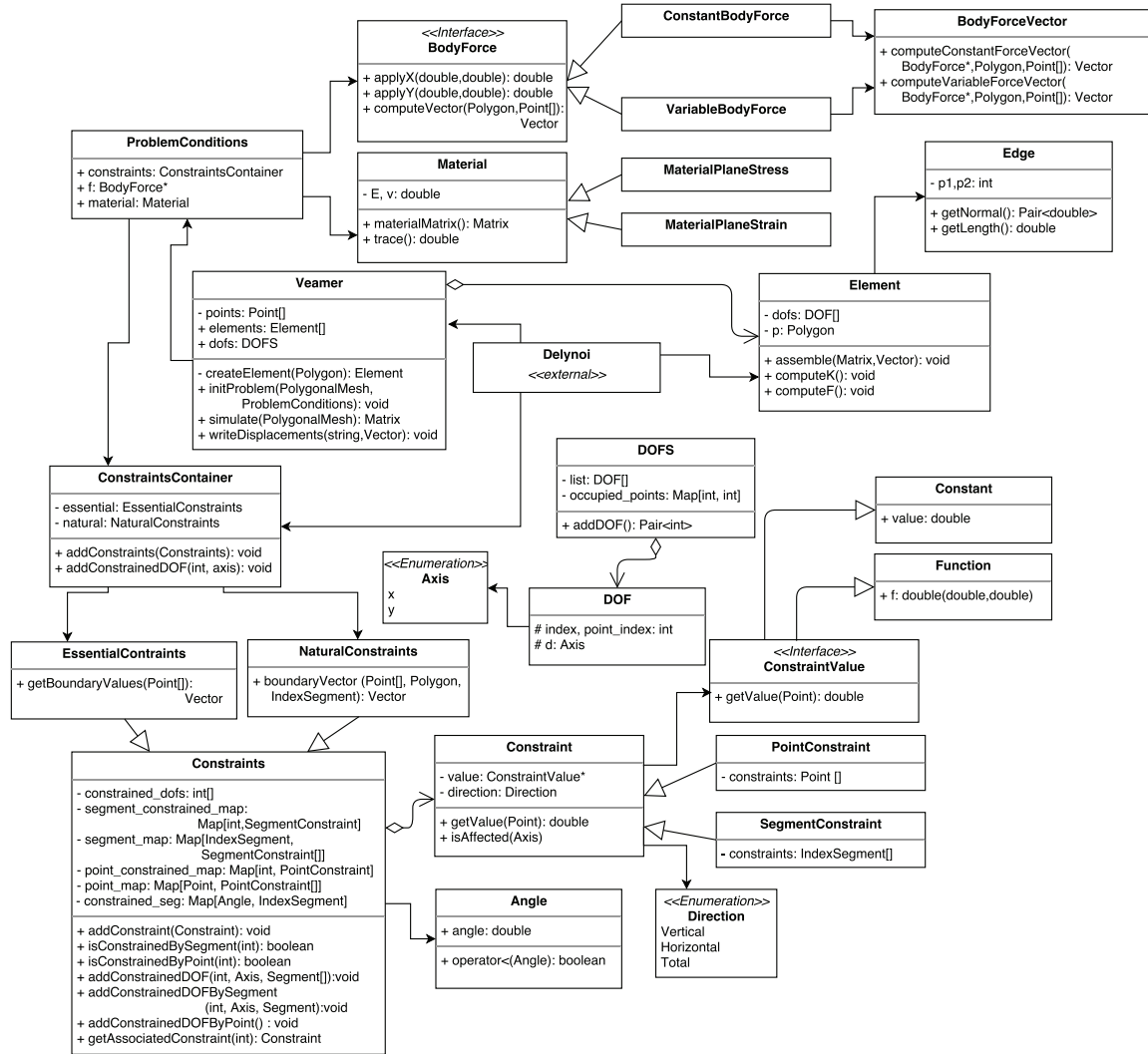


Fig. 2: UML diagram for the Veamy library.

4.1.2. *DOF*

`DOF`, is a class that represents the degrees of freedom associated with the nodal points. In the two-dimensional linear elastostatic problem, each nodal point of the mesh has two `DOF` instances associated that represent the components of the nodal displacement field in the Cartesian coordinate system. Since a nodal point is typically shared by various elements, to avoid memory overuse each `DOF` instance is kept only ones in a container class called `DOFS`, where the `DOF` instance is associated with its corresponding nodal point index. In addition, to facilitate the assembly of the element matrices into global ones, `DOFS` also assigns each `DOF` instance a global index that relates it to a specific row in the global stiffness matrix and global force vector.

4.1.3. *ProblemConditions*

`ProblemConditions` is a container structure that keeps the boundary conditions, the body force field, and the material properties of the two-dimensional linear elastic solid. `ProblemConditions` contains instances of three classes: `Material`, `BodyForce` and `ConstraintsContainer`.

4.1.4. *Material*

The current object-oriented VEM implementation considers a unique material definition for the entire domain, hence, we choose to represent the material properties as a class named `Material` along with two derived classes, `MaterialPlaneStrain` and `MaterialPlaneStress`. It contains the Young's modulus and the Poisson's ratio, which need to be set to compute the material constitutive matrix.

4.1.5. *BodyForce*

`BodyForce` is an interface that represents the VEM element body force vector. The `BodyForce` interface has three methods: `applyX`, `applyY` and `computeVector`. The first two are pure virtual functions that are meant to define a user-custom body force in the Cartesian coordinate system, and as such they must be implemented in a derived class. Both apply

methods receive two real numbers representing the x- and y-coordinate of an evaluation point, and return a single real. On the other hand, `computeVector` method is also a pure virtual function, but in contrast to `applyX` and `applyY`, is not expected to be implemented by the user, but rather is defined in two `BodyForce` subclasses: `ConstantBodyForce` and `VariableBodyForce`.

`ConstantBodyForce` is used for the computation of the VEM element body force vector when the body force is a constant field, in which case the helper class named `BodyForceVector`, through its method `computeConstantForceVector`, implements the exact integration presented in Section 3.9. `VariableBodyForce` is used when the body force is not a constant field, in which case the helper class `BodyForceVector`, through its method `computeVariableForceVector`, computes the VEM element body force vector using the nodal quadrature that is used in the computation of the volume integral in (29). This nodal quadrature is equivalent to the one presented in Gain et al. [14] to integrate the traction forces on the element faces.

The library includes one predefined zero body force implementation called `None`, which is used by default in absence of a user-custom body force function.

4.1.6. *EssentialConstraints and NaturalConstraints*

The essential (Dirichlet) and natural (Neumann) boundary conditions can be applied directly at boundary points and on boundary segments. After the mesh generation procedure, the essential boundary conditions will then be automatically translated to the corresponding nodes that lie at these points and on these segments.

The boundary conditions are grouped according to two parameters: their value and their kind (essential or natural). The former group is represented by a class called `Constraint` and two subclasses, named `SegmentConstraint` and `PointConstraint`, that contain a single value. This single value can be the outcome of imposing a constant value, which is represented by an instance of a class named `Constant`, or the outcome of a function, which is represented by an instance of a class named `Function`. Also, the class `Constraint`

stores the direction (in the Cartesian coordinate system) in which the constraint is applied, while `SegmentConstraint` and `PointConstraint` keep the segments and points where the constraint is applied, respectively. On the other hand, to assign a type to each constraint, two container classes called `NaturalConstraints` and `EssentialConstraints` are created as instances inside a container class named `ConstraintsContainer`. To avoid code duplication, we also include an abstract class named `Constraints`, which implements the operations that are common to both `NaturalConstraints` and `EssentialConstraints`.

Apart from providing a way of grouping the constraints, `ConstraintContainer` is also in charge of relating the constraints to the degrees of freedom of nodes that lie at points and on segments where the constraints are applied. For this purpose, when requested, the `addConstrainedDOF` method adds them to either the `NaturalConstraints` or `EssentialConstraints`.

`NaturalConstraints` is also the responsible for creating the VEM element traction force vector. This is done by its method `boundaryVector`.

4.1.7. *Element*

This class defines a single polygonal element. It contains as class field, the list of indexes of its degrees of freedom, its element stiffness matrix, its element body force vector, its element traction force vector, and the polygon this element represents. `Element` is in charge of:

1. creating the `DOF` object that contains the degrees of freedom associated with the element.
2. computing the VEM element stiffness matrix using the `computeK` method.
3. computing the VEM element force vector, which is the sum of the VEM element body force vector and the VEM element traction force vector. This operation is performed by `computeF` method.

4. assembling the VEM element stiffness matrix and the VEM element force vector into the global stiffness matrix and the global force vector, respectively. This operation is performed by `assemble` method.

As an example, Algorithm 1 summarizes the implementation of the VEM element stiffness matrix in the `Element` class using the notation presented in Sections 3.7 and 3.8.

Algorithm 1 Implementation of the VEM element stiffness matrix in the `Element` class.

$\mathbf{H}_{\mathcal{R}} = \mathbf{0}, \mathbf{W}_{\mathcal{R}} = \mathbf{0}, \mathbf{H}_{\mathcal{C}} = \mathbf{0}, \mathbf{W}_{\mathcal{C}} = \mathbf{0}$

for each node in the polygonal element **do**

Get incident edges

Compute the unit outward normal vector to each incident edge

Compute $(\mathbf{H}_{\mathcal{R}})_a$ and $(\mathbf{H}_{\mathcal{C}})_a$, and insert them into $\mathbf{H}_{\mathcal{R}}$ and $\mathbf{H}_{\mathcal{C}}$, respectively

Compute $(\mathbf{W}_{\mathcal{R}})_a$ and $(\mathbf{W}_{\mathcal{C}})_a$, and insert them into $\mathbf{W}_{\mathcal{R}}$ and $\mathbf{W}_{\mathcal{C}}$, respectively

end

Compute $\mathbf{I}_{2N}, \mathbf{P}_{\mathcal{R}}, \mathbf{P}_{\mathcal{C}}, \mathbf{P}_{\mathcal{P}}, \mathbf{D}$

Compute \mathbf{S}_E

Output: $\mathbf{K}_E = |E| \mathbf{W}_{\mathcal{C}} \mathbf{D} \mathbf{W}_{\mathcal{C}}^T + (\mathbf{I}_{2N} - \mathbf{P}_{\mathcal{P}})^T \mathbf{S}_E (\mathbf{I}_{2N} - \mathbf{P}_{\mathcal{P}})$

4.2. Computation of nodal displacements

Each simulation is represented by a single `Veamer` instance, which is in charge of conducting the VEM simulation through its `simulate` method until the displacement solution is obtained. The procedure is similar to a finite element simulation. The implementation of the `simulate` method is summarized in Algorithm 2.

Algorithm 2 Implementation of the `simulate` method in the `Veamer` class.

```
Initialization of global stiffness matrix and global force vector

for each element in the mesh do
    | Compute the element stiffness matrix
    | Compute the element force vector
    | Assemble the element stiffness matrix and the element force vector into global
    |   ones
end

Impose the essential boundary conditions into the global matrix system

Solve the resulting global matrix system of linear equations

Output: Column vector containing the nodal displacements solution
```

In structured programming, the input for the Algorithm 2 would be the mesh. However, in our object-oriented implementation the mesh is always known by the element. Hence, the mesh is not declared as an input in Algorithm 2.

The resulting matrix system of linear equations is solved using appropriate solvers available in the Eigen library [15] for linear algebra.

5. Sample usage

This section illustrates the usage of `Veamy` through several examples. For each example, a main C++ file is written to setup the problem. This is the only file that needs to be written by the user in order to run a simulation in `Veamy`. All the setup files for the examples that are considered in this section are included in the folder “`Veamy/test/.`” To be able to run these examples, it is necessary to compile the source code. A tutorial manual that provides complete instructions on how to prepare, compile and run the examples is included in the folder “`Veamy/docs/.`”

5.1. Cantilever beam subjected to a parabolic end load

The VEM solution for the displacement field on a cantilever beam of unit thickness subjected to a parabolic end load P is computed using **Veamy**. Fig. 3 illustrates the geometry and boundary conditions. Plane strain condition is assumed. The essential boundary conditions on the clamped edge are applied according to the analytical solution given by Timoshenko and Goodier [32]:

$$u_x = -\frac{Py}{6\overline{E}_Y I} \left((6L - 3x)x + (2 + \overline{\nu})y^2 - \frac{3D^2}{2}(1 + \overline{\nu}) \right),$$

$$u_y = \frac{P}{6\overline{E}_Y I} (3\overline{\nu}y^2(L - x) + (3L - x)x^2),$$

where $\overline{E}_Y = E_Y / (1 - \nu^2)$ with the Young's modulus set to $E_Y = 1 \times 10^7$ psi, and $\overline{\nu} = \nu / (1 - \nu)$ with the Poisson's ratio set to $\nu = 0.3$; $L = 8$ in. is the length of the beam, $D = 4$ in. is the height of the beam, and I is the second-area moment of the beam section. The total load on the traction boundary is $P = -1000$ lbf.

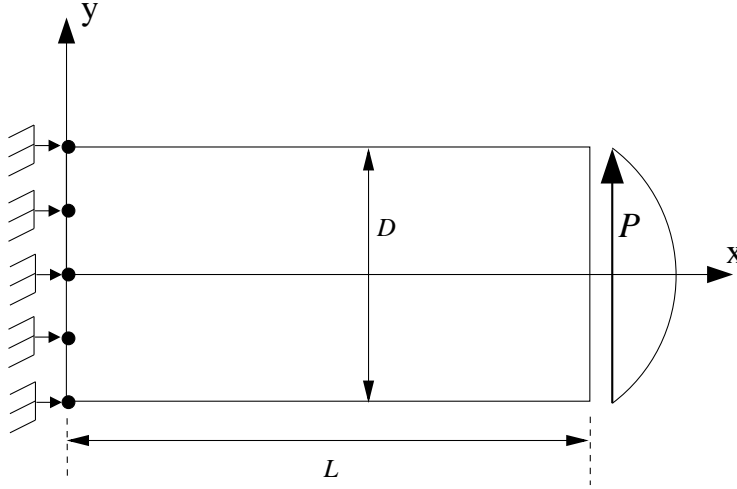


Fig. 3: Model geometry and boundary conditions for the cantilever beam problem.

5.1.1. Setup file

A main C++ file is written to setup the problem. As there are different aspects to consider, we divide the setup file in several blocks and explain each of them. Herein only the main parts of this setup file are described. The complete setup instructions for this problem are provided in the file “ParabolicMain.cpp” that is located in the folder “Veamy/test/.”

Listing 1 shows the definition of the problem domain, the generation of base points for the Voronoi diagram, and the computation of the polygonal mesh.

```
1  std::vector<Point> rectangle4x8_points = {Point(0, -2), Point(8, -2), Point(8, 2), Point(0, 2)};
2  Region rectangle4x8(rectangle4x8_points);
3  rectangle4x8.generateSeedPoints(PointGenerator(functions::constantAlternating(), functions::
    constant()), 24, 12);
4
5  std::vector<Point> seeds = rectangle4x8.getSeedPoints();
6  TriangleMeshGenerator meshGenerator = TriangleMeshGenerator (seeds, rectangle4x8);
7  PolygonalMesh mesh = meshGenerator.getMesh();
```

Listing 1: Geometry definition and mesh generation for the beam subjected to a parabolic end load.

We proceed to initialize all the structures needed to represent the conditions of the problem at hand. In first place, we create a constraint that represents the essential boundary condition that is imposed on the left side of the beam, including the segment it affects, the value of the constraint and the direction (in the Cartesian coordinate system) in which the constraint is imposed. This implementation is shown in Listing 2.

```
1  double uX(double x, double y){
2      double P = -1000;
3      double Ebar = 1e7/(1 - std::pow(0.3,2));
4      double vBar = 0.3/(1 - 0.3);
5      double D = 4; double L = 8; double I = std::pow(D,3)/12;
6      return -P*y/(6*Ebar*I)*((6*L - 3*x)*x + (2+vBar)*std::pow(y,2) - 3*std::pow(D,2)/2*(1+vBar));
```

```

7  }
8
9  double uY(double x, double y){
10     double P = -1000;
11     double Ebar = 1e7/(1 - std::pow(0.3,2));
12     double vBar = 0.3/(1 - 0.3);
13     double D = 4; double L = 8; double I = std::pow(D,3)/12;
14     return P/(6*Ebar*I)*(3*vBar*std::pow(y,2)*(L-x) + (3*L-x)*std::pow(x,2));
15 }
16 EssentialConstraints essential;
17 Function* uXConstraint = new Function(uX);
18 Function* uYConstraint = new Function(uY);
19
20 PointSegment leftSide(Point(0,-2), Point(0,2));
21 SegmentConstraint const1 (leftSide, mesh.getPoints(), Constraint::Direction::Horizontal,
    uXConstraint);
22 essential.addConstraint(const1, mesh.getPoints());
23
24 SegmentConstraint const2 (leftSide, mesh.getPoints(), Constraint::Direction::Vertical,
    uYConstraint);
25 essential.addConstraint(const2, mesh.getPoints());

```

Listing 2: Definition of the essential boundary condition on the left side of the beam.

Listing 3 presents the implementation of the natural boundary condition (the parabolic load) that is applied on the right side of the beam. The parabolic load is constructed using a function called `tangencial`.

```

1  double tangencial(double x, double y){
2     double P = -1000; double D = 4;
3     double I = std::pow(D,3)/12;
4     double value = std::pow(D,2)/4-std::pow(y,2);
5     return P/(2*I)*value;
6  }
7  NaturalConstraints natural;
8  Function* tangencialLoad = new Function(tangencial);
9

```

```

10 PointSegment rightSide(Point(8,-2), Point(8,2));
11 SegmentConstraint const3 (rightSide, mesh.getPoints(), Constraint::Direction::Vertical,
    tangencialLoad);
12 natural.addConstraint(const3, mesh.getPoints());

```

Listing 3: Definition of the natural boundary condition on the right side of the beam.

The `EssentialConstraints` and `NaturalConstraints` objects are inserted into an object of the `ConstraintContainer` class. An object of the `Material` class is created with the desired properties. The `ConstraintContainer` and `Material` objects are used to create a `ProblemConditions` object. The `ProblemConditions` object along with the mesh is used to initiate a `Veamer` instance that represents the system. Finally, to obtain the nodal displacements solution the `simulate` method is invoked. These instructions are presented in Listing 4.

```

1 ConstraintsContainer container;
2 container.addConstraints(essential, mesh);
3 container.addConstraints(natural, mesh);
4
5 Material* material = new MaterialPlaneStrain(1e7, 0.3);
6 ProblemConditions conditions(container, material);
7 Veamer veamer;
8 veamer.initProblem(mesh, conditions);
9 Eigen::VectorXd displacements = veamer.simulate(mesh);

```

Listing 4: Application of boundary conditions, material definition and assignment, and simulation for the beam subjected to a parabolic end load.

The output of the library is a column vector that contains the nodal displacements solution. To plot the nodal displacements solution to an output file it suffices to include an extra line after the `simulate` call. This line is shown in Listing 5. This instruction generates a text file that is named as the string stored in `displacementsFileName`. The text file contains the computed displacements in the following format: nodal index, x-

displacement and y-displacement. An extract of the output file generated for the beam subjected to a parabolic end load is shown in Listing 6.

```
1 veamer.writeDisplacements(displacementsFileName, displacements);
```

Listing 5: Plot nodal displacements solution to an output file.

1	0	9.38002e-005	-0.000100889
2	1	0.000137003	-0.000101589
3	2	9.30384e-005	-0.000115664
4	...		

Listing 6: Extract of the output file for the beam subjected to a parabolic end load.

The output file contains no information about the geometry of the problem. The geometry information is kept in the `PolygonalMesh` instance created at the beginning of the example. `PolygonalMesh` includes a method to print its geometrical data to a text file with a single line of code, as shown in Listing 7.

```
1 mesh.printInFile(meshFileName);
```

Listing 7: Print mesh data to a text file.

The text file containing the mesh information is named as the string stored in `meshFileName` and is arranged in the following format:

- **First line:** Number of nodal points in the polygonal mesh.
- **Following lines:** x-coordinate y-coordinate for each nodal point in the mesh.
- **One line:** Number of element edges in the polygonal mesh.
- **Following lines:** index-of-start-point index-of-end-point for each element edge in the polygonal mesh.

- **One line:** Number of polygons in the polygonal mesh.
- **Following lines:** number-of-element-nodes list-of-nodal-indexes centroid-x-coordinate centroid-y-coordinate for each polygon in the mesh.

5.1.2. Post processing

Veamy does not provide a post processing interface. The user may opt to use a post processing interface of their choice. In the present example, we have chosen to visualize the displacement results using a MATLAB function written for this purpose. This MATLAB function is provided in the folder “Veamy/lib/visualization/” as the file “plot-PolyMeshDisplacements.m.” Fig. 4(a)-(c) present the VEM solutions, and for reference, Fig. 4(d) presents the norm of the exact solution.

5.2. Patch test

In this example, the polygonal mesh for the beam problem studied in Section 5.1 is used to test **Veamy** on a displacement patch test, which consists in the solution of the linear elastostatic problem with Dirichlet boundary conditions $\mathbf{g} = \{x_1 \quad x_1 + x_2\}^T$ imposed along the entire boundary, and $\mathbf{b} = \mathbf{0}$. Plane strain condition is assumed with the following material parameters: $E_Y = 1 \times 10^7$ psi and $\nu = 0.3$. The complete setup instructions for this problem are provided in the file “DisplacementPatchTestMain.cpp” that is located in the folder “Veamy/test/.” As predicted by the theory, the VEM solution coincides with the exact solution, which is given by \mathbf{g} , within machine precision. The results are shown in Fig. 5, where the norm of the displacement error is shown in letter (d).

5.3. Using a *PolyMesher* mesh and boundary conditions in *Veamy*

A polygonal mesher that is widely used in the VEM and polygonal finite elements communities is **PolyMesher** [30]. **PolyMesher** delivers a polygonal mesh along with nodal displacements constraints and prescribed nodal loads. It is coded in MATLAB.

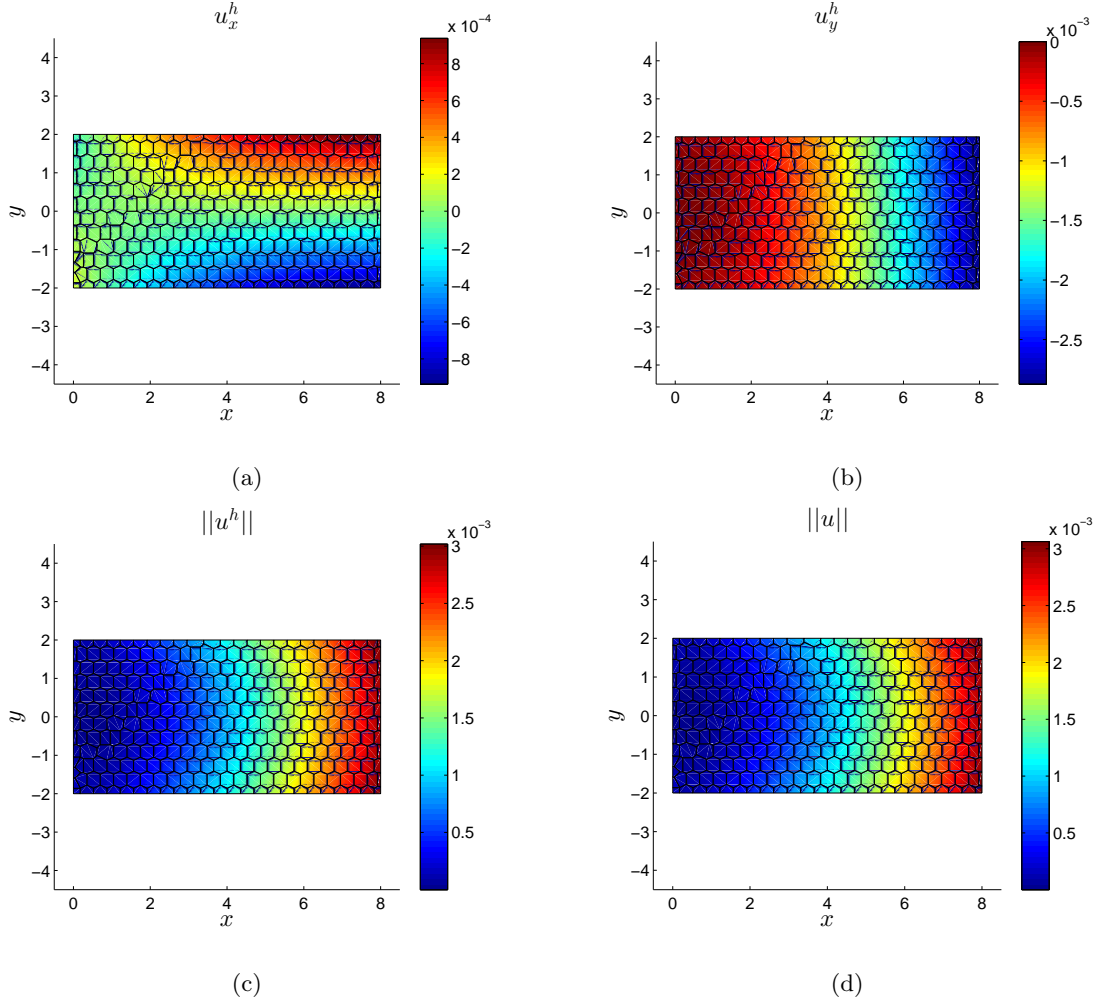


Fig. 4: Solution for the cantilever beam subjected to a parabolic end load using **Veamy**. (a) VEM horizontal displacement, (b) VEM vertical displacement, (c) norm of the VEM displacement, and (d) norm of the exact displacement.

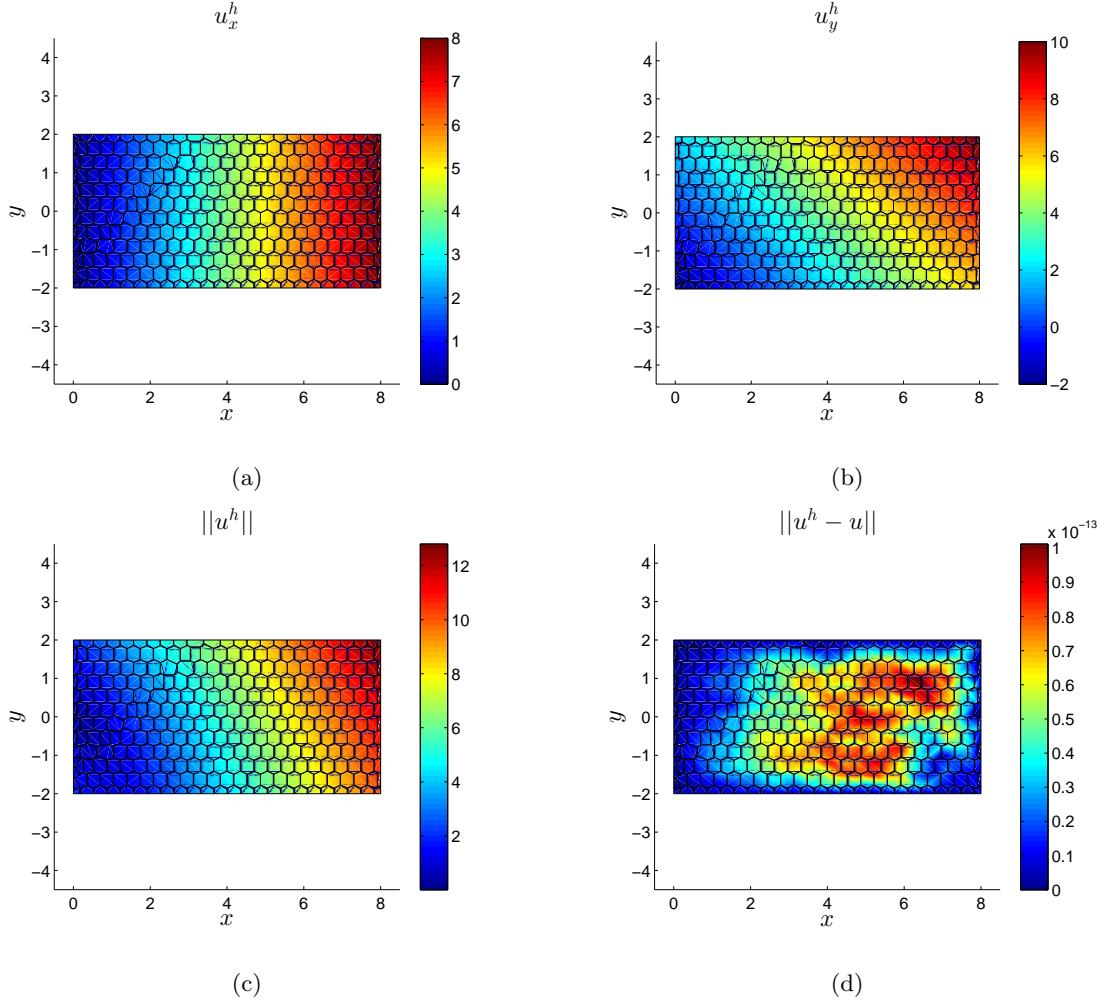


Fig. 5: Solution for the displacement patch test using **Veamy**. (a) VEM horizontal displacement, (b) VEM vertical displacement, (c) norm of the VEM displacement, and (d) norm of the VEM displacement error.

In order to conduct a simulation in **Veamy** using data stemming from **PolyMesher**, a MATLAB function named **PolyMesher2Veamy**, which needs to be called from **PolyMesher**, was especially devised to read these data and write them to a text file in a format that is readable by **Veamy**. This MATLAB function is provided in the folder “**Veamy/poly-mesher/.**” Function **PolyMesher2Veamy** receives five **PolyMesher**’s data structures (**Node**, **Element**, **NElem**, **Supp**, **Load**) and writes a text file containing the mesh and boundary conditions. **Veamy** implements a function named **initProblemFromFile** that is able to read this text file and solve the problem straightforwardly.

As a demonstration of the potential that is offered to the simulation when **Veamy** interacts with **PolyMesher**, the MBB beam problem of Section 6.1 in Ref. [30] is considered. The MBB problem is shown in Fig. 6, where $L = 3$ in, $D = 1$ in and $P = 0.5$ lbf. The following material parameters are considered: $E_Y = 1 \times 10^7$ psi, $\nu = 0.3$ and plane strain condition is assumed. The polygonal mesh and boundary conditions created in **PolyMesher** are shown in Fig. 7. The MATLAB function **PolyMesher2Veamy** is used to read the polygonal mesh and boundary conditions from **PolyMesher** and write them to the text file “**polymesher2veamy.txt.**” This text file is provided in the folder “**Veamy/test/test_files/.**” The complete setup instructions for this problem are provided in the file “**PolyMesherMain.cpp**” that is located in the folder “**Veamy/test/.**” Finally, the VEM solution for the MBB beam problem that is obtained using **Veamy** is presented in Fig. 8.

5.4. *Perforated Cook’s membrane*

In this example, a perforated Cook’s membrane is considered. The objective of this problem is to show more advanced geometry definition and mesh generation capabilities offered by **Veamy**. The model geometry, polygonal mesh and boundary conditions are shown in Fig. 9. The following material parameters are considered: $E_Y = 250$ MPa, $\nu = 0.3$ and plane strain condition is assumed. The complete setup instructions for this problem are provided in the file “**CookTestMain.cpp**” that is located in the folder “**Veamy/test/.**” The

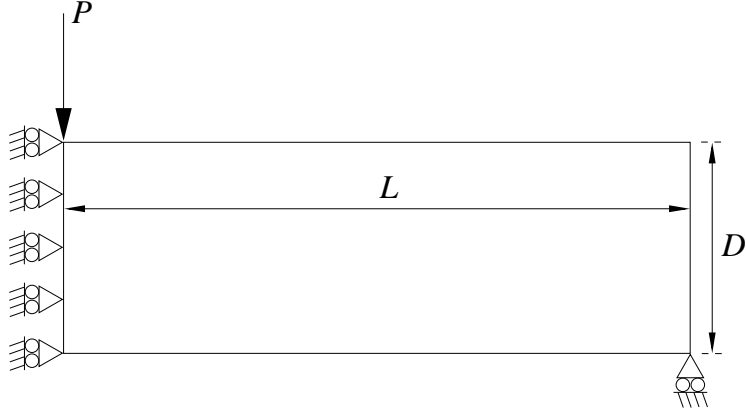


Fig. 6: MBB beam problem definition as per Section 6.1 in Ref. [30].

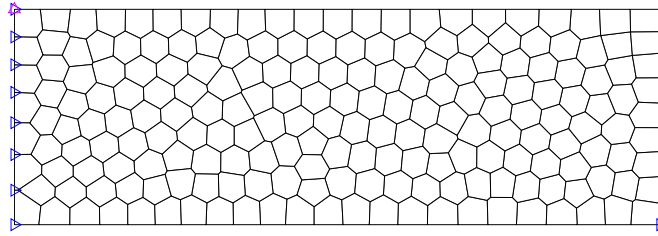


Fig. 7: Polygonal mesh and boundary conditions generated in PolyMesher for the MBB beam problem.

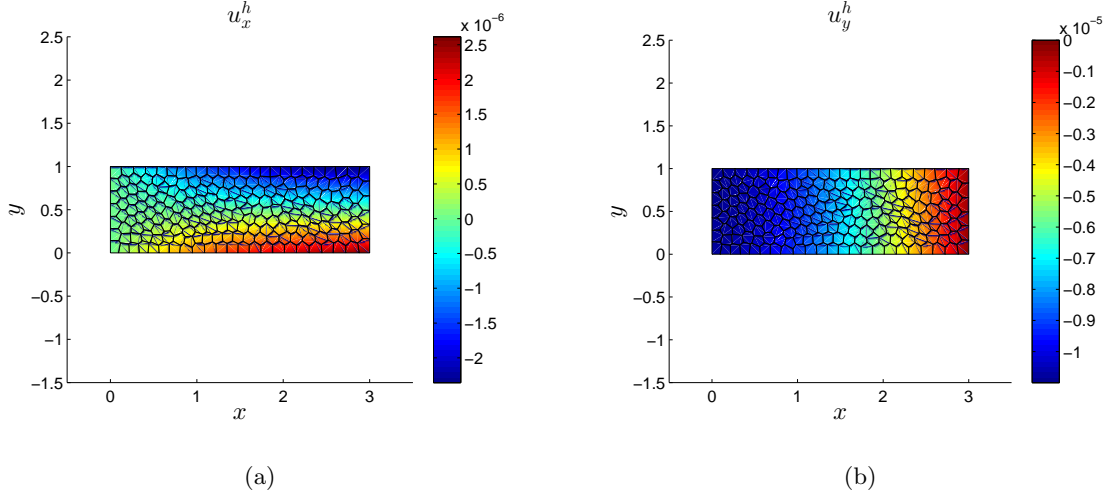


Fig. 8: Solution for the MBB beam problem using **Veamy**. (a) VEM horizontal displacement and (b) VEM vertical displacement.

VEM solution for the perforated Cook’s membrane problem that is obtained using **Veamy** is presented in Fig. 10.

5.5. A toy problem

We conclude the examples with a toy problem consisting in a Unicorn loaded on its back and fixed at its feet. The objective of this problem is to show additional capabilities for the geometry definition and mesh generation that are available in **Veamy**. The model geometry, polygonal mesh and boundary conditions are shown in Fig. 11. The following material parameters are considered: $E_Y = 1 \times 10^4$ psi, $\nu = 0.25$ and plane strain condition is assumed. The complete setup instructions for this problem are provided in the file “UnicornTestMain.cpp” that is located in the folder “Veamy/test/.” The VEM solution that is obtained using **Veamy** is presented in Fig. 12.

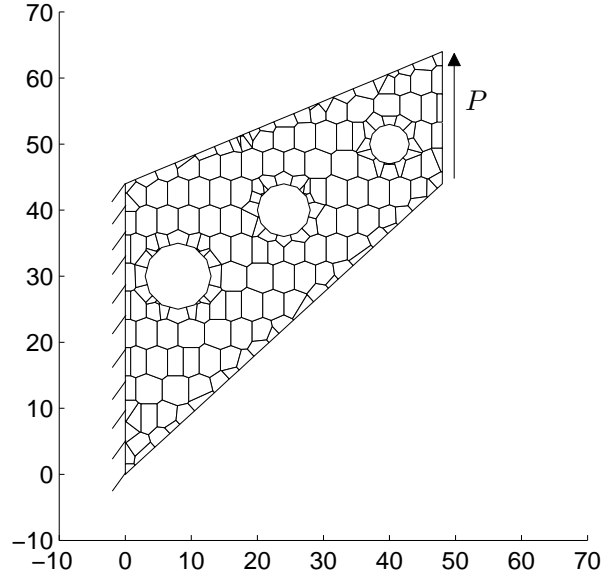


Fig. 9: Model geometry, polygonal mesh and boundary conditions for the perforated Cook's membrane problem.

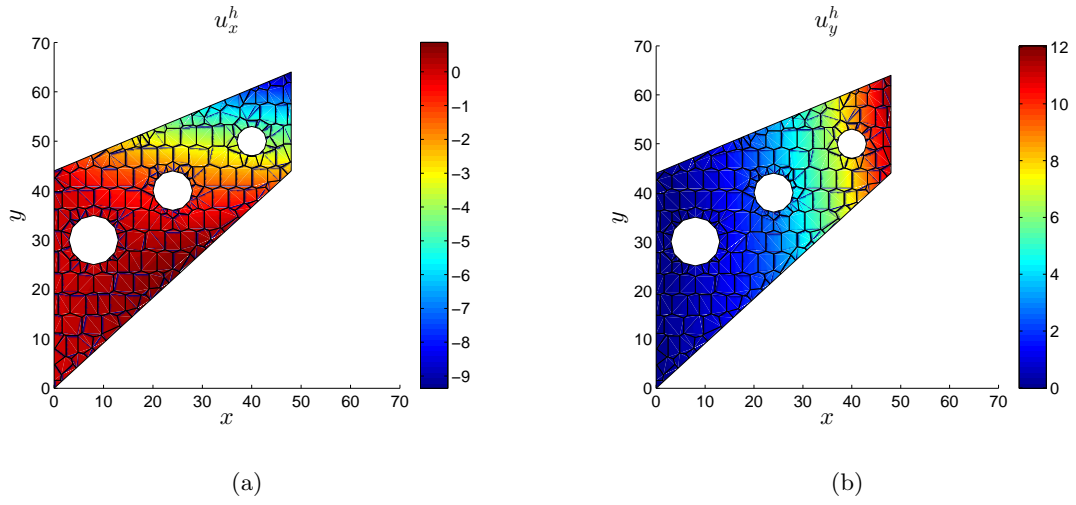


Fig. 10: Solution for the perforated Cook's membrane problem using **Veamy**. (a) VEM horizontal displacement and (b) VEM vertical displacement.

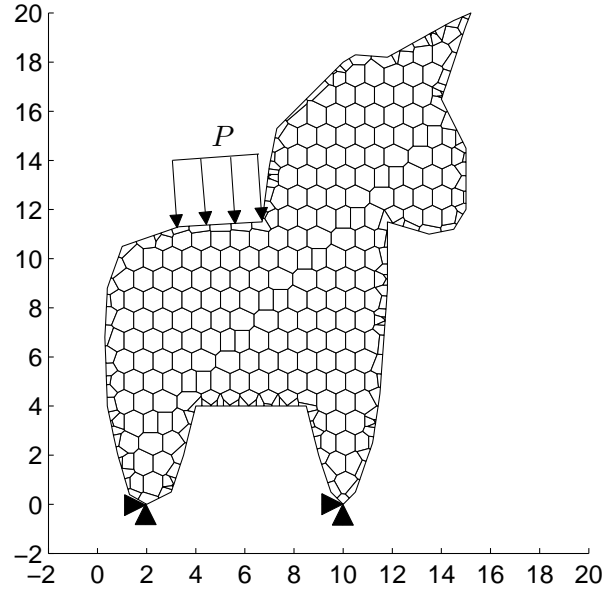


Fig. 11: Model geometry, polygonal mesh and boundary conditions for the toy problem.

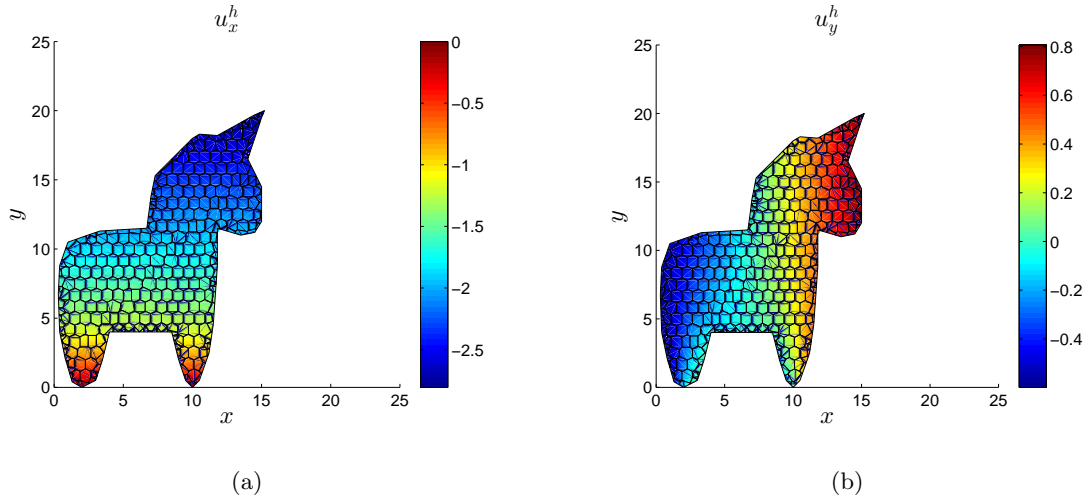


Fig. 12: Solution for the toy problem using **Veamy**. (a) VEM horizontal displacement and (b) VEM vertical displacement.

6. Concluding remarks

In this paper, an object-oriented programming of the virtual element method in two-dimensional linear elastostatics has been presented. As a result, a C++ VEM library named **Veamy** has been developed. A stepwise sample usage of this library, which consisted in the solution of the displacement field of a cantilever beam subjected to a parabolic end load, has been provided. **Veamy** was also tested on a displacement patch test and a demonstration of its interaction with **PolyMesher** was featured. In just a few lines of code, **Veamy** can straightforwardly solve any linear elastostatic problem using a **PolyMesher** mesh and boundary conditions. Two additional examples, namely a perforated Cook’s membrane and a toy problem consisting in a Unicorn loaded on its back and fixed at its feet, were presented to demonstrate more advanced capabilities available in **Veamy** for geometry definition and polygonal mesh generation. To the best of our knowledge, **Veamy** is the first object-oriented C++ implementation of the VEM. Possible extensions of this library that are of interest include the solution of three-dimensional linear elastostatic problems, where an interaction with the polyhedral mesh generator Voro++ [25] seems very appealing, and although recently introduced, the solution of nonlinear solid mechanics problems [3, 8, 36, 37]. We have made **Veamy** a free and open source software.

Appendix A Demonstration of some properties and relations used in the VEM derivations

It is instructive to demonstrate some crucial properties and relations that were used in previous sections. In all of the demonstrations that follow, we consider the definitions for $\Pi_0 \mathbf{v}$, $\Pi_{\mathcal{P}} \mathbf{v}$, $\Pi_{\mathcal{R}} \mathbf{v}$ and $\Pi_{\mathcal{C}} \mathbf{v}$ given in (30), (33), (34) and (35), respectively.

We start by verifying the orthogonality condition given in (14).

Proof. From (6) and (35), we have

$$\omega(\mathbf{c}) = \nabla_{\text{AS}}(\Pi_{\mathcal{C}} \mathbf{c}) = \frac{1}{2} (\nabla \Pi_{\mathcal{C}} \mathbf{c} - \nabla^T \Pi_{\mathcal{C}} \mathbf{c}) = \frac{1}{2} (\widehat{\varepsilon}(\mathbf{c}) - \widehat{\varepsilon}(\mathbf{c})) = 0,$$

which by (26) implies that $\widehat{\boldsymbol{\omega}}(\boldsymbol{c}) = 0$. In addition, $\overline{\boldsymbol{c}} = \overline{\Pi_{\mathcal{C}} \boldsymbol{c}} = \widehat{\boldsymbol{\varepsilon}}(\boldsymbol{c}) \cdot (\overline{\boldsymbol{x}} - \overline{\boldsymbol{x}}) = 0$. Therefore, from (34) and the preceding results,

$$\Pi_{\mathcal{R}} \boldsymbol{c} = \widehat{\boldsymbol{\omega}}(\boldsymbol{c}) \cdot (\boldsymbol{x} - \overline{\boldsymbol{x}}) + \overline{\boldsymbol{c}} = \widehat{\boldsymbol{\omega}}(\boldsymbol{c}) \cdot (\boldsymbol{x} - \overline{\boldsymbol{x}}) + \overline{\Pi_{\mathcal{C}} \boldsymbol{c}} = 0.$$

□

We also verify the orthogonality condition (15).

Proof. From (34), $\nabla \Pi_{\mathcal{R}} \boldsymbol{r} = \widehat{\boldsymbol{\omega}}(\boldsymbol{r})$. And since $\widehat{\boldsymbol{\omega}}(\boldsymbol{r})$ is a skew-symmetric tensor, it follows that $\nabla^T \Pi_{\mathcal{R}} \boldsymbol{r} = -\widehat{\boldsymbol{\omega}}(\boldsymbol{r})$. These results lead to

$$\nabla_S(\Pi_{\mathcal{R}} \boldsymbol{r}) = \frac{1}{2} (\nabla \Pi_{\mathcal{R}} \boldsymbol{r} + \nabla^T \Pi_{\mathcal{R}} \boldsymbol{r}) = \frac{1}{2} (\widehat{\boldsymbol{\omega}}(\boldsymbol{r}) - \widehat{\boldsymbol{\omega}}(\boldsymbol{r})) = 0.$$

Therefore, from (35) and (25), the preceding result, and observing that $\boldsymbol{\varepsilon}(\boldsymbol{r}) = \nabla_S(\boldsymbol{r}) = \nabla_S(\Pi_{\mathcal{R}} \boldsymbol{r})$, we obtain

$$\Pi_{\mathcal{C}} \boldsymbol{r} = \widehat{\boldsymbol{\varepsilon}}(\boldsymbol{r}) \cdot (\boldsymbol{x} - \overline{\boldsymbol{x}}) = \left(\frac{1}{|E|} \int_E \nabla_S(\Pi_{\mathcal{R}} \boldsymbol{r}) \, d\boldsymbol{x} \right) \cdot (\boldsymbol{x} - \overline{\boldsymbol{x}}) = 0.$$

□

It was also stated that the rigid body modes have zero strain, which in fact follows from the preceding proof as

$$\boldsymbol{\varepsilon}(\boldsymbol{r}) = \nabla_S(\boldsymbol{r}) = \nabla_S(\Pi_{\mathcal{R}} \boldsymbol{r}) = 0$$

and

$$\boldsymbol{\varepsilon}(\Pi_{\mathcal{R}} \boldsymbol{v}) = \nabla_S(\Pi_{\mathcal{R}} \boldsymbol{v}) = \frac{1}{2} (\widehat{\boldsymbol{\omega}}(\boldsymbol{v}) - \widehat{\boldsymbol{\omega}}(\boldsymbol{v})) = 0.$$

The next demonstration is tailored to verify that the energy-orthogonality condition (18) is satisfied for $\Pi_{\mathcal{C}} \boldsymbol{v}$ given in (35).

Proof. From (5) and (35), we have

$$\boldsymbol{\varepsilon}(\Pi_{\mathcal{C}} \boldsymbol{v}) = \nabla_S(\Pi_{\mathcal{C}} \boldsymbol{v}) = \frac{1}{2} (\nabla \Pi_{\mathcal{C}} \boldsymbol{v} + \nabla^T \Pi_{\mathcal{C}} \boldsymbol{v}) = \frac{1}{2} (\widehat{\boldsymbol{\varepsilon}}(\boldsymbol{v}) + \widehat{\boldsymbol{\varepsilon}}(\boldsymbol{v})) = \widehat{\boldsymbol{\varepsilon}}(\boldsymbol{v}).$$

On using (7) at element level, (25) along with the preceding result, and noting that $\boldsymbol{\sigma}(\mathbf{c})$ and $\widehat{\boldsymbol{\varepsilon}}(\mathbf{v})$ are tensors with constant components, we get

$$\begin{aligned}
a_E(\mathbf{c}, \mathbf{v} - \Pi_C \mathbf{v}) &= \boldsymbol{\sigma}(\mathbf{c}) : \left[\int_E \boldsymbol{\varepsilon}(\mathbf{v}) \, d\mathbf{x} - \int_E \boldsymbol{\varepsilon}(\Pi_C \mathbf{v}) \, d\mathbf{x} \right] \\
&= \boldsymbol{\sigma}(\mathbf{c}) : \left[\int_E \boldsymbol{\varepsilon}(\mathbf{v}) \, d\mathbf{x} - \int_E \widehat{\boldsymbol{\varepsilon}}(\mathbf{v}) \, d\mathbf{x} \right] \\
&= \boldsymbol{\sigma}(\mathbf{c}) : \left[\int_E \boldsymbol{\varepsilon}(\mathbf{v}) \, d\mathbf{x} - \widehat{\boldsymbol{\varepsilon}}(\mathbf{v}) \int_E d\mathbf{x} \right] \\
&= \boldsymbol{\sigma}(\mathbf{c}) : \left[\int_E \boldsymbol{\varepsilon}(\mathbf{v}) \, d\mathbf{x} - \widehat{\boldsymbol{\varepsilon}}(\mathbf{v}) |E| \right] \\
&= \boldsymbol{\sigma}(\mathbf{c}) : \left[\int_E \boldsymbol{\varepsilon}(\mathbf{v}) \, d\mathbf{x} - \int_E \boldsymbol{\varepsilon}(\mathbf{v}) \, d\mathbf{x} \right] = 0.
\end{aligned}$$

□

Finally, we show that (30) satisfies the orthogonality condition (28).

Proof.

$$\begin{aligned}
\Pi_0(\mathbf{v} - \Pi_P \mathbf{v}) &= \overline{\mathbf{v}} - \Pi_P \overline{\mathbf{v}} \\
&= \overline{\mathbf{v}} - (\Pi_R \overline{\mathbf{v}} + \Pi_C \overline{\mathbf{v}}) \\
&= \overline{\mathbf{v}} - (\widehat{\boldsymbol{\omega}}(\overline{\mathbf{v}}) \cdot (\mathbf{x} - \overline{\mathbf{x}}) + \overline{\mathbf{v}} + \widehat{\boldsymbol{\varepsilon}}(\overline{\mathbf{v}}) \cdot (\mathbf{x} - \overline{\mathbf{x}})) \\
&= \overline{\mathbf{v}} - \overline{\mathbf{v}} = 0,
\end{aligned}$$

where it has been used that $\widehat{\boldsymbol{\omega}}(\overline{\mathbf{v}}) = \widehat{\boldsymbol{\varepsilon}}(\overline{\mathbf{v}}) = 0$ since $\overline{\mathbf{v}}$ is a vector with constant components.

□

Acknowledgments

AOB acknowledges the support provided by Universidad de Chile through the “Programa VID Ayuda de Viaje 2017.” The work of CA is supported by CONICYT-PCHA/Magíster Nacional/2016-22161437. NHK is grateful for the support provided by Proyecto Enlace VID 009/15.

References

- [1] Delynoi v1.0. <https://github.com/capalvarez/Delynoi> (2017)
- [2] Alnæs, M.S., Blechta, J., Hake, J., Johansson, A., Kehlet, B., Logg, A., Richardson, C., Ring, J., Rognes, M.E., Wells, G.N.: The FEniCS Project Version 1.5. Arch. Numer. Softw. **3**(100), 9–23 (2015)
- [3] Artioli, E., Beirão da Veiga, L., Lovadina, C., Sacco, E.: Arbitrary order 2D virtual elements for polygonal meshes: part II, inelastic problem. Comput. Mech. **0**(0), 0 (2017). DOI 10.1007/s00466-017-1429-9
- [4] Babuška, I., Banerjee, U., Osborn, J.E., Li, Q.L.: Quadrature for meshless methods. Int. J. Numer. Meth. Engng. **76**(9), 1434–1470 (2008)
- [5] Babuška, I., Banerjee, U., Osborn, J.E., Zhang, Q.: Effect of numerical integration on meshless methods. Comput. Methods Appl. Mech. Engng. **198**(37–40), 2886–2897 (2009)
- [6] Cangiani, A., Manzini, G., Russo, A., Sukumar, N.: Hourglass stabilization and the virtual element method. Int. J. Numer. Meth. Engng. **102**(3–4), 404–436 (2015)
- [7] Chen, J.S., Wu, C.T., Yoon, S., You, Y.: A stabilized conforming nodal integration for Galerkin mesh-free methods. Int. J. Numer. Meth. Engng. **50**(2), 435–466 (2001)
- [8] Chi, H., Beirão da Veiga, L., Paulino, G.: Some basic formulations of the virtual element method (VEM) for finite deformations. Comput. Methods Appl. Mech. Engng. **318**, 148–192 (2017)
- [9] Dolbow, J., Belytschko, T.: Numerical integration of Galerkin weak form in meshfree methods. Comput. Mech. **23**(3), 219–230 (1999)
- [10] Duan, Q., Gao, X., Wang, B., , Li, X., Zhang, H., Belytschko, T., Shao, Y.: Consistent element-free Galerkin method. Int. J. Numer. Meth. Engng. **99**(2), 79–101 (2014)

- [11] Duan, Q., Gao, X., Wang, B., Li, X., Zhang, H.: A four-point integration scheme with quadratic exactness for three-dimensional element-free Galerkin method based on variationally consistent formulation. *Comput. Methods Appl. Mech. Engrg.* **280**(0), 84–116 (2014)
- [12] Duan, Q., Li, X., Zhang, H., Belytschko, T.: Second-order accurate derivatives and integration schemes for meshfree methods. *Int. J. Numer. Meth. Engng.* **92**(4), 399–424 (2012)
- [13] Francis, A., Ortiz-Bernardin, A., Bordas, S., Natarajan, S.: Linear smoothed polygonal and polyhedral finite elements. *Int. J. Numer. Meth. Engng.* **109**(9), 1263–1288 (2017)
- [14] Gain, A.L., Talischi, C., Paulino, G.H.: On the virtual element method for three-dimensional linear elasticity problems on arbitrary polyhedral meshes. *Comput. Methods Appl. Mech. Engrg.* **282**(0), 132–160 (2014)
- [15] Guennebaud, G., Jacob, B., et al.: Eigen v3. <http://eigen.tuxfamily.org> (2010)
- [16] Hecht, F.: New development in FreeFem++. *J. Numer. Math.* **20**(3–4), 251–265 (2012)
- [17] Johnson, A.: Clipper - an open source freeware library for clipping and offsetting lines and polygons (version: 6.1.3). <http://www.angusj.com/delphi/clipper.php> (2014)
- [18] Manzini, G., Russo, A., Sukumar, N.: New perspectives on polygonal and polyhedral finite element methods. *Math. Models Methods Appl. Sci.* **24**(08), 1665–1699 (2014)
- [19] Ortiz, A., Puso, M.A., Sukumar, N.: Maximum-entropy meshfree method for compressible and near-incompressible elasticity. *Comput. Methods Appl. Mech. Engrg.* **199**(25–28), 1859–1871 (2010)

- [20] Ortiz, A., Puso, M.A., Sukumar, N.: Maximum-entropy meshfree method for incompressible media problems. *Finite Elem. Anal. Des.* **47**(6), 572–585 (2011)
- [21] Ortiz-Bernardin, A., Hale, J.S., Cyron, C.J.: Volume-averaged nodal projection method for nearly-incompressible elasticity using meshfree and bubble basis functions. *Comput. Methods Appl. Mech. Engrg.* **285**, 427–451 (2015)
- [22] Ortiz-Bernardin, A., Puso, M.A., Sukumar, N.: Improved robustness for nearly-incompressible large deformation meshfree simulations on Delaunay tessellations. *Comput. Methods Appl. Mech. Engrg.* **293**, 348–374 (2015)
- [23] Ortiz-Bernardin, A., Russo, A., Sukumar, N.: Consistent and stable meshfree Galerkin methods using the virtual element decomposition. *Int. J. Numer. Meth. Engng.* (2017). DOI 10.1002/nme.5519
- [24] PrudHomme, C., Chabannes, V., Doyeux, V., Ismail, M., Samake, A., Pena, G.: Feel++: A computational framework for Galerkin methods and advanced numerical methods. In: *ESAIM: Proceedings*, vol. 38, pp. 429–455. EDP Sciences (2012)
- [25] Rycroft, C.H.: Voro++: A three-dimensional Voronoi cell library in C++. *Chaos* **19** (2009)
- [26] Shewchuk, J.R.: Triangle: Engineering a 2D Quality Mesh Generator and Delaunay Triangulator. In: M.C. Lin, D. Manocha (eds.) *Applied Computational Geometry: Towards Geometric Engineering, Lecture Notes in Computer Science*, vol. 1148, pp. 203–222. Springer-Verlag (1996). From the First ACM Workshop on Applied Computational Geometry
- [27] Strang, G., Fix, G.: *An Analysis of the Finite Element Method*, second edn. Wellesley-Cambridge Press, MA (2008)

- [28] Sutton, O.J.: The virtual element method in 50 lines of MATLAB. *Numer. Algor.* **75**(4), 1141–1159 (2017)
- [29] Talischi, C., Paulino, G.H.: Addressing integration error for polygonal finite elements through polynomial projections: A patch test connection. *Math. Models Methods Appl. Sci.* **24**(08), 1701–1727 (2014)
- [30] Talischi, C., Paulino, G.H., Pereira, A., Menezes, I.F.M.: PolyMesher: a general-purpose mesh generator for polygonal elements written in Matlab. *Struct. Multidisc. Optim.* **45**(3), 309–328 (2012)
- [31] Talischi, C., Pereira, A., Menezes, I., Paulino, G.: Gradient correction for polygonal and polyhedral finite elements. *Int. J. Numer. Meth. Engng.* **102**(3–4), 728–747 (2015)
- [32] Timoshenko, S.P., Goodier, J.N.: *Theory of Elasticity*, third edn. McGraw-Hill, NY (1970)
- [33] Beirão da Veiga, L., Brezzi, F., Cangiani, A., Manzini, G., Marini, L.D., Russo, A.: Basic principles of virtual element methods. *Math. Models Methods Appl. Sci.* **23**(1), 199–214 (2013)
- [34] Beirão da Veiga, L., Brezzi, F., Marini, L.D.: Virtual elements for linear elasticity problems. *SIAM J. Numer. Anal.* **51**(2), 794–812 (2013)
- [35] Beirão da Veiga, L., Brezzi, F., Marini, L.D., Russo, A.: The Hitchhiker’s Guide to the Virtual Element Method. *Math. Models Methods Appl. Sci.* **24**(08), 1541–1573 (2014)
- [36] Beirão da Veiga, L., Lovadina, C., Mora, D.: A virtual element method for elastic and inelastic problems on polytope meshes. *Comput. Methods Appl. Mech. Engrg.* **295**, 327–346 (2015)

- [37] Wriggers, P., Reddy, B.D., Rust, W., Hudobivnik, B.: Efficient virtual element formulations for compressible and incompressible finite deformations. *Comput. Mech.* **0**(0), 0 (2017). DOI 10.1007/s00466-017-1405-4